7. RESPONSE MODIFICATION DESIGN

7.1 Introduction

The concept of seismic isolation has been known from the early days, however it started to be implemented in the last three decades. Considerable progress of structural analysis using computers made it possible to implement the seismic isolation. Since evaluation of nonlinear response resulting from the hysteretic behavior of isolators and dampers is essential, systematic application of seismic isolation was difficult until nonlinear dynamic response analysis technologies became available.

Development of reliable hardware consisting of various materials and mechanisms was also important. In particular, development of the lead-rubber bearings contributed implementation of seismic isolation worldwide (Robinson and Greenbank 1976, Robinson 1982, Skinner, Robinson, McVerry 1993).

Unique technical developments for seismic response modification have been conducted in Japan for bridge application. Since most destructive seismic damage of bridges has occurred as a result of failure of ground and foundations, an emphasis has been placed on the mitigation of damage in foundations. It was the 1970s when an early concept of response modification using viscous damper stoppers was initiated to implement. Technologies that enabled to construct multi-span continuous viaducts in urban areas were required. Variety of technologies was developed for long-span bridges, in particular cable-stayed bridges.

Use of the lead-rubber bearings and the high-damping rubber bearings have made it possible to systematically implement the seismic isolation in the 1990s. A design procedure with limiting the increase of natural period, which is known as Menshin Design, was developed in mid-1990s. The Kobe Earthquake has accelerated the implementation of seismic isolation.

This chapter shows the past and current practice of response modification of highway bridges.

7.2 Response Modification using Viscous Damper Stoppers

Mitigation of seismic damage to structures is a dream for structural engineers; hence a wide range of technical development has been attempted for response modification from 1970s. An early application of the response modification was underlaid by a philosophy that a technology that enabled to construct multi-span continuous bridges, without controlled by the thermal, creep and shrinkage effects, was required. Viscous dampers were often incorporated in bridge in the 1970s.

Since viscous fluid with viscosity nearly free from the temperature dependence was not available at the early days, high viscosity fluid was used in the dampers so that the dampers resist high rate seismic movement, while they do not resist low rate movement resulting from the thermal, creep and shrinkage effects. Consequently dampers have been effectively used to distribute seismic lateral force of a superstructure to substructures, with relative displacements resulting from the thermal, creep and shrinkage effects being allowed to take place without restriction. It is thus called “viscous damper stopper.” Energy is not dissipated in the viscous damper stoppers. Photos 1 and 2 show an example of the implementation of the viscous damper stoppers. The standard piston-cylinder type dampers are used in this example. Photo 7.3 shows a shear viscous damper stopper (for example, Fukuda 1980, Iseki 1980). Steel plates spaced with an equal interval are saturated by a viscous fluid. Since a half of the steel plates are connected to a top plate and the other half steel plates are connected to a bottom plate, a viscous shear force is induced when this stopper is shear between the top and the bottom plates.

Photo 7.1 Viaduct with Viscous Damper Stoppers, Metropolitan Expressway

Photo 7.2 Viscous Damper Stoppers

SU-Damper consists of sliding bearings and prestressed strands as shown in Photos 7.4 and 7.5. It was used in the 1970s to construct multi-span continuous viaducts in urban areas. Sliding bearings dissipate energy with the natural period being controlled by prestressed strands between the deck and the substructures (Okamoto and Uemae 1963).

Photo 7.3 Viscous Damper Stopper

Photo 7.4 Viaduct with SU-Dampers, Metropolitan Expressway

Photo 7.5 Cables and Bearings for SU-Damper

7.3 Response Modification of Cable Stayed Bridges

Response modification has been effectively used in cable-stayed bridges. In a 758m long Meiko-Nishi Bridge, Nagoya, a steel box girder deck is free to oscillate in longitudinal direction with the natural period being controlled by prestressed cables (Kato, Iioka and Kawahito 1983) as shown in Photos 7.6 and 7.7. The prestressed cables prevent excessive deck displacement in an earthquake. As shown in Photos 7.8 and 7.9, tower links were used in the 860m long Yokohama-Bay Bridge, Metropolitan Expressway, for controlling the natural period and preventing excessive deck displacement. Two large plate-springs were provided at the end of the deck in the 790m long Hitsuishi Bridge, Honshu-Shikoku Bridges, as shown in Photos 7.10 and 11, for controlling the natural period (Kanemitsu and Higuchi 1981). Sixty-eight 32mm thick tapered steel plates were used to form a plate-spring. Rotating vane-type dampers were adopted in the 885m long Higashi-Kobe Bridge, Hanshin Expressway (Kitazawa, Iseki and Shimoda 1994) and the 1020m long Tsurumi-Tsubasa Bridge, Metropolitan Expressway (Enomoto et al 1994).

Photo 7.6 Meko-nishi Bridge, JH

Photo 7.7 Prestressed Cable in the Deck, Meiko-Nishi Bridge, JH

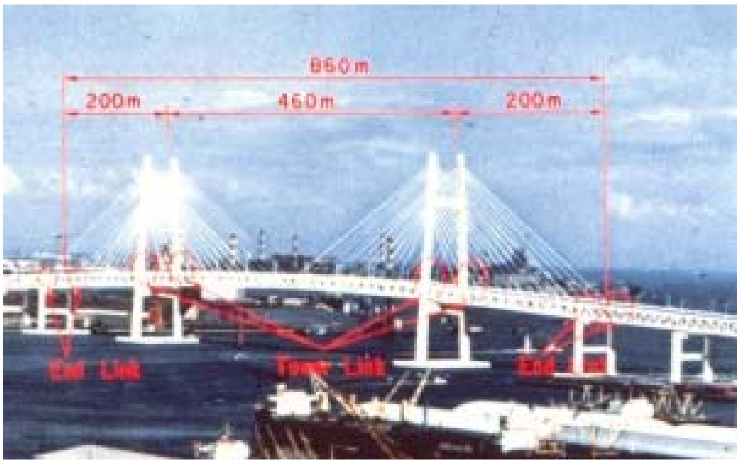

Photo 7.8 Yokohama-Bay Bridge, Metropolitan Expressway

Photo 7.9 Links used for Isolation of the Deck from Towers, Yokohama Bay Bridge

Photo 7.10 End Plate-Spring, Hitsuishi Bridge, Honshu-Shikoku Bridges

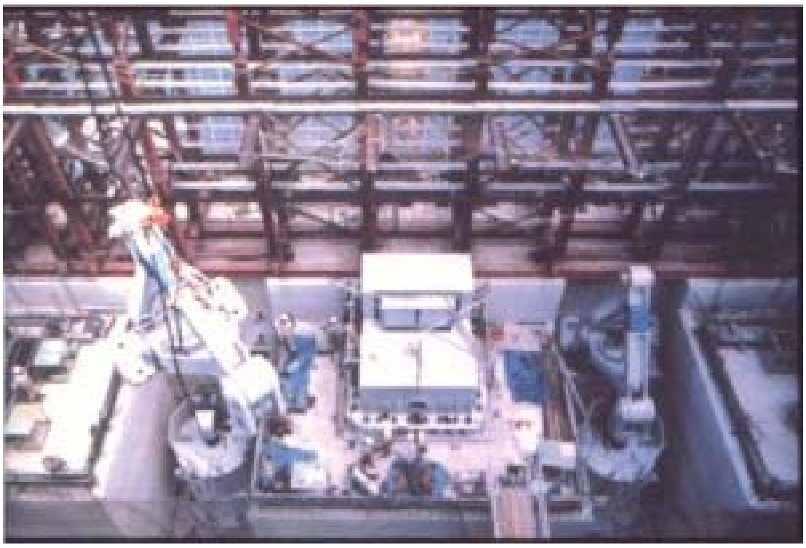

Photo 7.11 Installation of Two End Plate-Springs, Hitsuishi Bridge

Since steel bearings have been vulnerable to seismic disturbance and weak for corrosion, it has been recommended to replace steel bearings with elastomeric bearings. The first attempt to develop a methodology of seismic isolation was realized in 1989 in the form of the “Guideline for Seismic Isolation of Highway Bridges” (Technology Research Center for National Land Development 1989). Although it was not a mandate guideline, application of the seismic isolation to highway bridges was initiated at this time. Subsequently, a more comprehensive “Menshin Manual for Highway Bridges” was compiled in 1992 (Public Works Research

Institute 1992, Kawashima 1992, Kawashima 1994, Sugita and Mahin 1994). A consistent design procedure that takes account of response modification resulting from the hysteretic behavior of isolators and columns was developed. As will be described later, the limited increase of natural period was recommended in the Menshin Manual for Highway Bridges. It is called “Menshin Design.”

The destructive damage of bridges and viaducts in the 1995 Hyogo-ken Nanbu Earthquake has let to a marked increase of seismic isolation. Many reinforced concrete or steel piers did not performed as well as might be expected under the strong excitation. It was recommended in the reconstruction of the damaged bridges that seismic isolation (Menshin Design) should be used, wherever possible, for multi-span continuous bridges (Ministry of Construction 1995). The design procedure proposed in the 1992 Menshin Manual was used. It was subsequently incorporated in the 1996 Design Specifications of Highway Bridges (Japan Road Association 1996, Kawashima and Unjoh 1997, Kawashima 2000a). The lead rubber bearings and the high damping rubber bearings have been increasingly adopted since the Hyogo-ken Nanbu Earthquake.

7.4 Seismic Isolation

1) Principles

The period shift and the enhancement of energy dissipation capacity are the basic principles of seismic isolation (Skinner, Robinson and McVerry, 1993, Buckle and Mayes, 1992). As shown in Fig. 7.1, increasing the natural period from Point A to Point B brings the decrease of acceleration response. However this increase of natural period generally increases the response displacement of a deck. Consequently, if the damping ratio of a bridge system can be increased from ξ_1 to ξ_2, this reduces both the acceleration and displacement responses of the bridge from Point B to Point C. If the response displacement of a deck at Point C is in the acceptable level, the seismic isolation can b e implemented. However if the increasing of the natural period results in the resonance, and if the deck displacement at Point C is not still acceptable level, the seismic isolation should not be implemented.

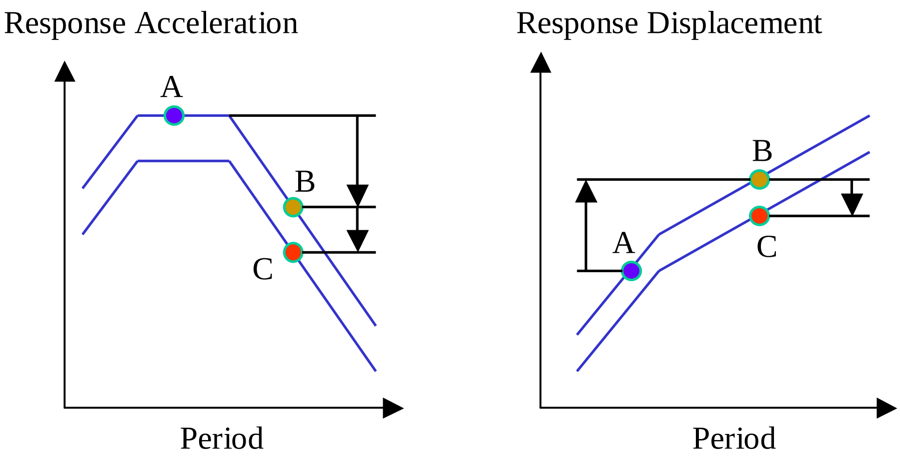

(a) Response Acceleration (b) Response Displacement

Fig. 7.1 Principle of Seismic Isolation

In the seismic isolation, particular attention has to be given to the increase of the natural period, because the period shift generally brings the increase of response displacement in a deck. For example, a 10m-high standard urban highway viaduct with a fixed-base natural period of about 0.8s may have the natural period of 1.5-2s when isolated, and response displacement of the deck may be in the range of 0.3-0.7m when subjected to the ground motions by Eqs. (6.2) and (6.3). Relative displacement between viaducts may be further amplified due to the phase delay.

Since the clearance between decks at an expansion joint is generally 0.1-0.3 in a standard bridge, the decks cannot displace as expected in a design earthquake, which results in insufficient increase of natural period and energy dissipation. Furthermore, such a large relative displacement would result in collisions between decks, which, in turn, causes excessive large lateral force to transfer from one deck to the other. It should be noted that expansion joints that accommodate large relative displacement is not desirable, because it causes vibration and noise problems as well as overwhelming maintenance in an urban area.

Hence in the application of seismic isolation to bridges and viaducts, it has been recommended that the natural period should not be excessively increased but that an emphasis should be placed for the increase of energy dissipation capacity and the distribution of seismic lateral force of a deck to as many piers as possible. The natural period of an isolated bridge has been recommended about twice the natural period of the fixed-base bridge. As described earlier, such a design practice has been called “Menshin Design.” It should be noted that inelastic hysteretic response might occur in piers in the Menshin Design because the natural period may not be sufficiently increased. The Menshin Design has been used as a design tool that enables to construct multi-span continuous bridges with the distribution of seismic lateral force to piers.

2) System Design

In the design of an isolated bridge, it is important to determine the system response first followed by the design of isolators. However since the system design inherently depends on the characteristics of isolators, an iteration process is generally required. It is common that an isolated bridge is first sized based on the inelastic static analysis, and then an inelastic dynamic response analysis is conducted to verify the overall performance.

In the inelastic static analysis, the equivalent lateral force F_{eq} has to be carefully evaluated accounting for the effects of increasing the natural periods and the energy dissipating capacity of an isolated bridge. It is preferable to concentrate the plastic deformation only at the isolators. Stiffness of the isolators has to be carefully determined so that sufficient increase of the natural period of the bridge from the fixed-base condition can be achieved. If the increase of the natural periods is not sufficient, the isolator and column interaction may occur, which results in the plastic deformation at not only the isolators but also the columns. In particular, the plastic deformation of columns is significant when the bridge is subjected to a long period ground acceleration.

For example, Fig. 7.2 shows the hystereses of the isolator and the column of a 10 m tall reinforced concrete bridge when it is subjected to the JMS Kobe observatory ground acceleration in the 1995 Kobe Earthquake (refer to Fig. 1.1 (a)). The bridge consists of a steel deck girder supported by 5 lead rubber bearings per column. Since the structural and soil conditions are nearly the same along the bridge axis, only a part of the superstructure and a column are analyzed. The fundamental natural period of the bridge under the fixed-base condition, T_F, is about 1 second. Stiffness of the isolators is modified so that they have the stiffness equivalent to *n/5* times the original stiffness, where *n* is varied from 2 to 10 in Fig. 7.2. It is preferable to set *n*=5 because most energy dissipated in the isolators with the column being nearly elastic. It is noted that much larger energy dissipation occurs in the column in the fixed-base condition. The peak deck displacement is 0.15 m in the fixed-base condition, while it is about 0.2 m in the isolated condition. This amount of displacement is not problem in design. Hence the seismic isolation is effective for this bridge under the JMA Kobe ground acceleration. It is noted that the energy dissipation in the column increase as *n* becomes 10. This is because

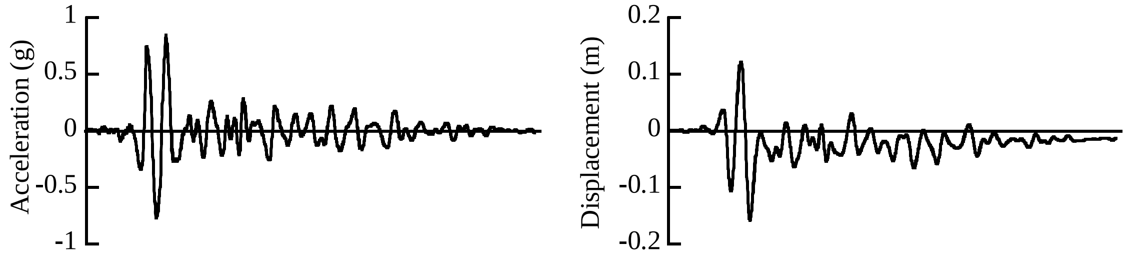

(a) Fixed-Base Bridge

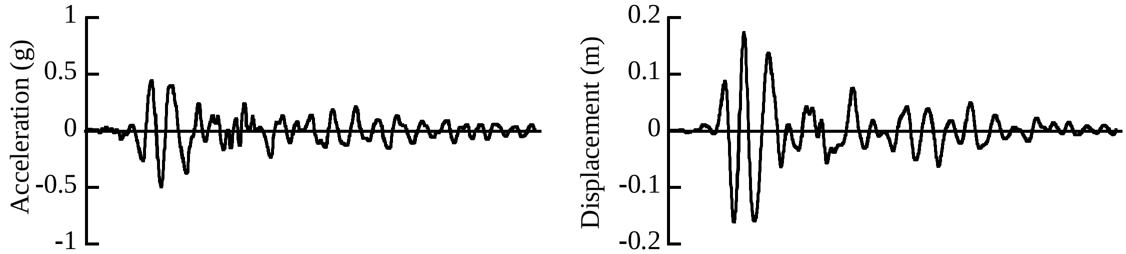

(b) Stiffness and Strength of Isolators are 2/5 x Standard Value

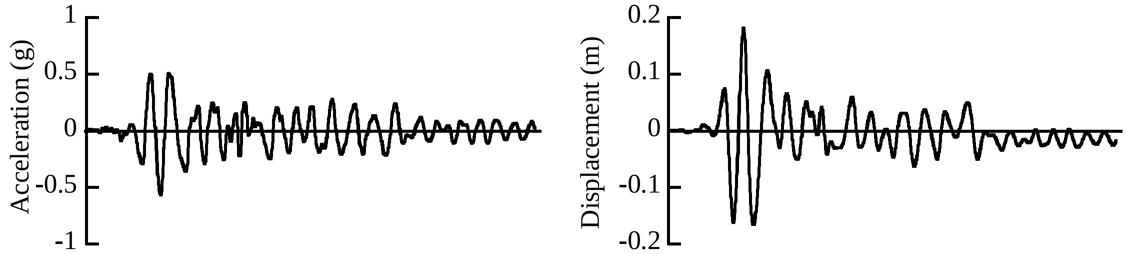

(c) Stiffness and Strength of Isolators are 5/5 x Standard Value

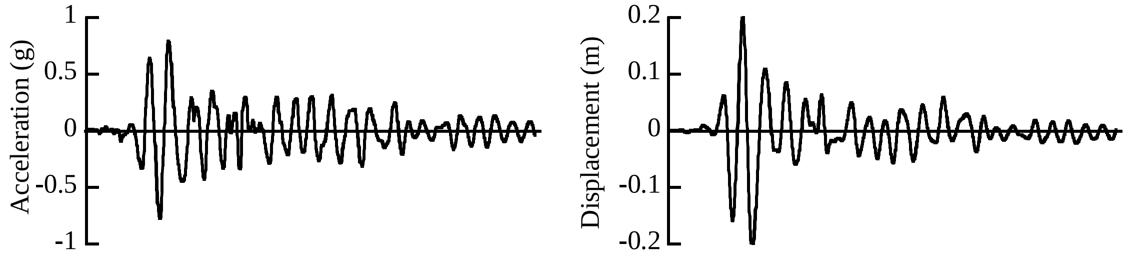

(d) Stiffness and Strength of Isolators are 7/5 x Standard Value

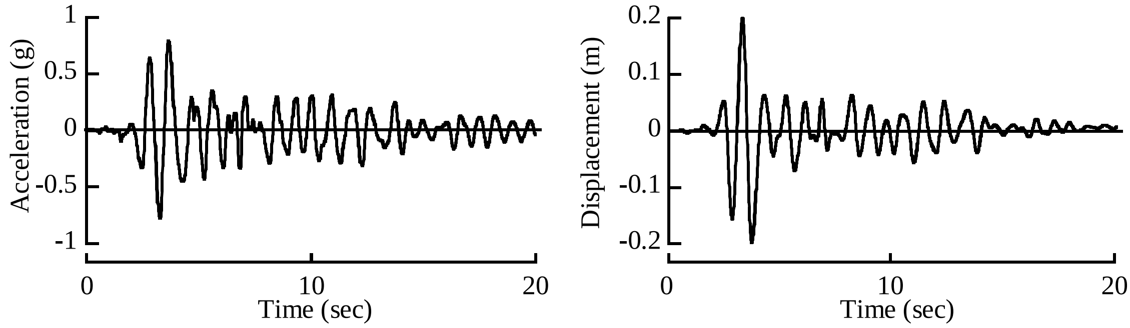

(e) Stiffness and Strength of Isolators are 10/5 x Standard Value

Fig. 7.2 Effect of Stiffness and Strength of the Isolators on the Hysteretic Response of the Isolators and the Column under the JMA Kobe Observatory Record

the excessive stiffness of the isolators results in decrease of the energy dissipation in the isolators.

One can define the energy dissipation in the columns as

$$U_C^I = \oint M_C^I d\theta_C^I \tag{7.1}$$

$$U_C^F = \oint M_C^F d\theta_C^F \tag{7.2}$$

in which U_C^I are U_C^F are the energy dissipation in the column in an isolated bridge and a fixed-base bridge, respectively, M_C^I and θ_C^I are the bending moment and rotation of the column in the isolated bridge, and M_C^F and θ_C^F are the bending moment and rotation of the column in the fixed-based bridge.

If one defines a ratio of energy dissipation of the column between then isolated bridge and the fixed-based bridge as

$$r_C = \frac{U_C^I}{U_C^F} \tag{7.3}$$

r_C should be sufficiently smaller than 1.0 if the seismic isolation is to be used. The ratio r_C is plotted in Fig. 7.3 for the bridge under the JMA Kobe ground motion described above. The ratio r_C is sufficiently small at the fundamental natural period T longer than 1.4 second, which implies that T/T_F of 1.3 is sufficient where T_F is the fundamental natural period of the fixed-based bridge.

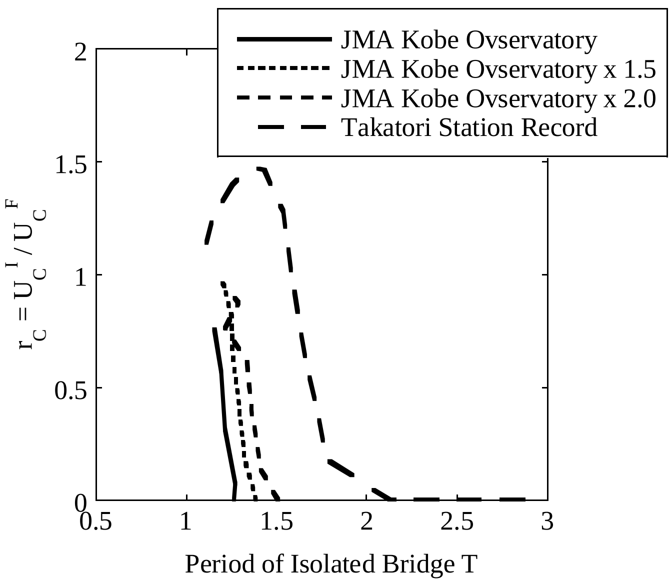

Fig. 7.3 Effect of Natural Period of Isolated Bridges on $r_C = U_C^I / U_C^F$ by Eq. (7.3)

However, it should be noted that an appropriate isolator stiffness depends on the ground motions. For example, Fig. 7.4 shows the hystereses of the isolators and the column in the same bridge that is subjected to JR Takatori ground acceleration. Since the Takatori acceleration has longer period components than the JMA Kobe acceleration, the energy dissipation in the column is still large at *n*=5-7. Consequently, the fundamental natural period T has to be longer than 2 second and T/T_F should be larger than about 2 as shown in Fig. 7.4. Period characteristics of the site-specific ground motion has to be carefully evaluated in the determination of seismic isolation. Since the deck displacement generally increases as the fundamental natural period increases, there must be another requirement for the fundamental natural period from the limitation of the peak deck displacement. It is recommended in the Design Specifications of Highway Bridges that the fundamental natural period is evaluated as

$$\frac{T}{T_F} \approx 2 \tag{7.4}$$

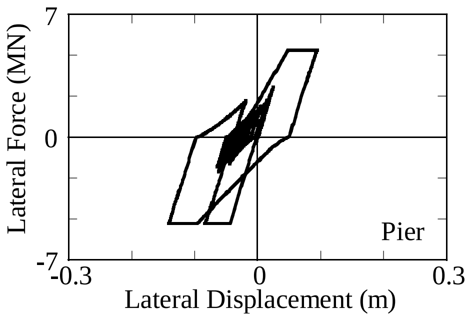

(a) Fixed-Base Bridge

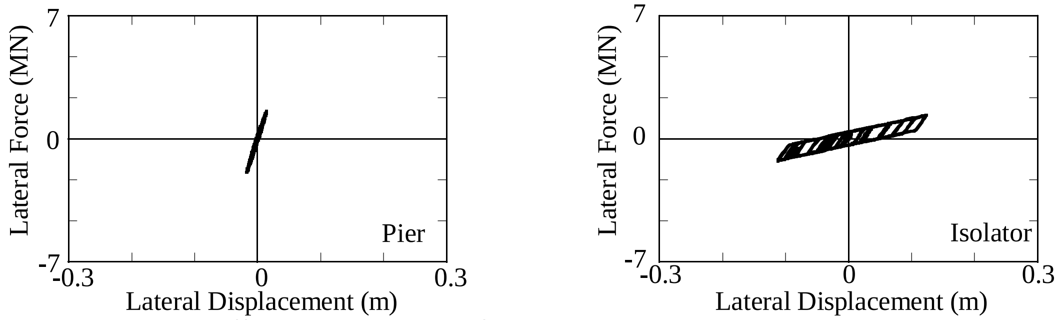

(b) Stiffness and Strength of Isolators are 2/5 x Standard Value

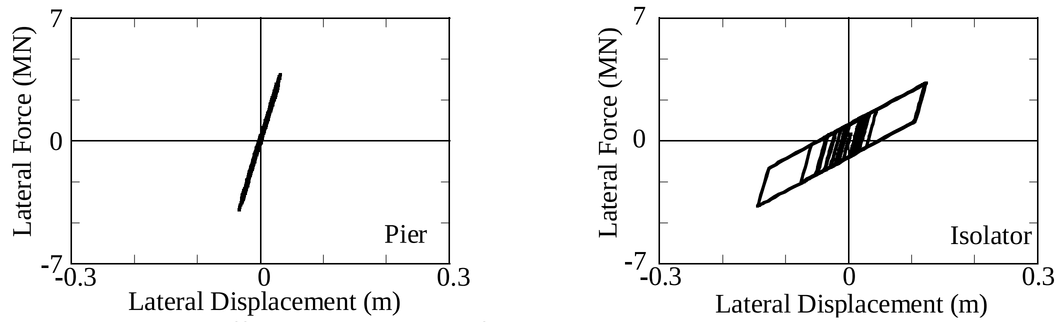

(c) Stiffness and Strength of Isolators are 5/5 x Standard Value

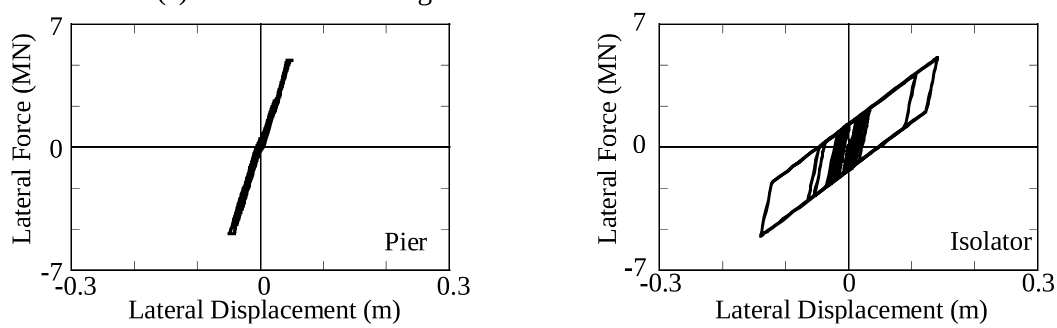

(d) Stiffness and Strength of Isolators are 7/5 x Standard Value

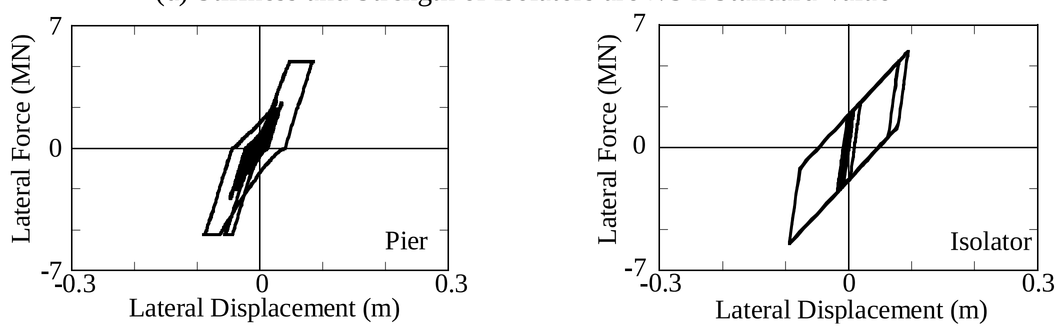

(e) Stiffness and Strength of Isolators are 10/5 x Standard Value

Fig. 7.4 Effect of Stiffness and Strength of the Isolators on the Hysteretic Response of the Isolators and the Column under the JR Takatori Record

Including the effect of inelastic response of columns, the equivalent static lateral force of an isolated bridge F_{eq} may be evaluated as

$$F_{eq} = \frac{F}{R_I} \tag{7.5}$$

where

$$R_I = R_E \cdot R_\mu \tag{7.6}$$

in which R_E is the response modification factor that accounts for the energy dissipation in the bridge system by dampers, and R_μ is the response modification factor that accounts for the inelastic response of piers. Obviously Eq. (7.6) is an approximated relation for separating the two effects. Since the two effects are coupled, they have to be evaluated by the inelastic dynamic response analysis.

The force reduction factor R_E may be evaluated from Eq. (1.23) as

$$R_E = c_D(\xi_I) \tag{7.7}$$

in which ξ_I is the damping ratio of an isolated bridge for the fundamental mode. The damping ratio of an isolated bridge may be evaluated by Eq. (2.6) based on the equivalent damping ratio of isolators.

The force reduction factor R_μ may be approximately evaluated by Eq. (1.44) as

$$R_\mu = \begin{cases} \sqrt{2\mu_I - 1} & \text{equal energy} \\ \mu_\mathrm{I} & \text{equal displacement} \end{cases} \tag{7.8}$$

in which μ_I is the response displacement ductility factor of a column.

In the Japanese seismic design specifications, R_E in Eq. (7.7) is provided as shown in Table 7.1 depending on the fundamental natural period of an isolated bridge. The force reduction factor as high as 1.43 is used in design of highway bridges. On the other hand, the force reduction factor R_μ by q. (7.8) is evaluated in design as

$$R_\mu = \sqrt{2\mu_{Ia} - 1} \tag{7.9}$$

in which μ_{Ia} is the design displacement ductility factor of the column, and is given as

$$\mu_{Ia} = 1 + \frac{u_u - u_y}{\alpha_I \cdot u_y} \tag{7.10}$$

in which u_y and u_u: yield and ultimate displacement of a pier, and α_I is safety factor for a column in an isolated bridge. The safety factor α_I is given as

$$\alpha_I = 2\alpha \tag{7.11}$$

in which α is the safety factor for a column in a fixed-based bridge (refer to Table 6.?). Eq. (7.11) intends to limit the hysteretic behavior of columns in an isolated bridge than the fixed-based bridge. The use the design displacement ductility factor in stead of the response ductility factor of a column is for avoiding the iteration in the design process.

Table 7.1 Response Modification Factor depending on Energy Dissipation Capacity R_E

First-mode Damping Ratio ξ_I	Response Modification Factor R_E
$\xi_I < 0.1$	1.0
$0.1 \le \xi_I < 0.12$	1.11
$0.12 \le \xi_I < 0.15$	1.25

$0.15 \le \xi_I$	1.43

3) Design of Devices

It is important that isolators and energy dissipaters are stable within the displacement rage of the design displacement, and they should be replaceable when damaged. They are designed for a target design displacement u_B as

$$u_B = \frac{F_{eq}}{K_B} \tag{7.12}$$

in which F_{eq} is the equivalent lateral force in the inelastic static analysis by Eq. (9), and K_B is the equivalent stiffness of a device. The equivalent stiffness K_B and the equivalent damping ratio ξ_B of a device are defined as

$$K_B = \frac{F_B(u_{Be}) - F(-u_{Be})}{2u_{Be}} \tag{7.13}$$

$$\xi_B = \frac{\Delta W}{2\pi W} \tag{7.14}$$

where,

$$u_{Be} = c_B \cdot u_B \tag{7.15}$$

in which $F_B(u)$: restoring force of a device at displacement of u , u_{Be} : equivalent displacement, c_B: coefficient to evaluate the effective displacement (= 0.7), ΔW : energy dissipation of a device per cycle, and W : elastic strain energy.

In design of devices, the following requirements have to be satisfied:

- Displacement of a devise computed by Eq. (7.12) should be within +/-10% from the assumed design displacement u_B, and the equivalent damping ratio evaluated by Eq. (7.14) should not be less than the equivalent damping ratio assumed in design.
- Shear strain in an elastomeric bearing γ_B subjected to the equivalent lateral force F_{eq} defined as

$$\lambda_B \equiv \frac{u_B}{\sum_{r=1}^{n} t_{ri}} \tag{7.16}$$

  should be less than 250%, in which u_B is the design displacement by Eq. (7.12), t_{ri} is the thickness of i-th rubber layer, and n is the number of rubber layers.
- Local shear strain should be less than the rupture strain divided by a factor of 1.2.
- Devices have to be designed and fabricated so that scatter of the equivalent stiffness K_B and the equivalent damping ratio ξ_B are within 10% of the design values.
- Devices have to be stable for at least 50 and 15 lateral load reversals with the design displacements u_B by Eq. (7.12) for the Type-I and Type-II ground motions, respectively, under a vertical static load equivalent to the tributary weight.
- To prevent “shake-down,” tangential stiffness of a device should be positive at any displacement within the design displacement u_B.
- A deck should return to the rest position after it is subjected to design ground motions. Residual displacement u_{BR} developed in a device after it is smoothly released from a deformed displacement equivalent to the design displacements u_B should be less than 10% of the design displacement.
- The equivalent stiffness K_B and the equivalent damping ratio ξ_B should be stable for a

change of load conditions and natural environment including the thermal extension of a deck.

7.5 Implementation of Seismic Isolation

1) Application to a 29-span Continuous Viaduct

a) Ohito Viaduct

O-Hito Viaduct is a 1.929km long 66-span viaduct as shown in Photo 7.12. It is a part of National Highway 135 in Izu Peninsula. It is separated into 5 segments (7, 29, 15, 3 and 12 span continuous viaducts). Application of the seismic isolation is presented here for a 725m long 29-span continuous viaduct (Matsuno, Hara and Yamashita 1994). A reinforced concrete hollow slab deck with a 29m long span (25m x 29-span = 725m) is supported by 4 lead rubber bearings per pier. The lead-rubber bearings were 230.8mm tall (thickness of rubber was 13mm@10 layers), and the size was 580mm x 580mm at the end piers (refer to Photo 7.13) and 680mm x 680mm at the intermediate piers. Unseating prevention devices as shown in Photo 7.14 were provided at the end of the deck to prevent excessive displacement. 7.5m tall reinforced concrete piers support the deck as shown in Photo 7.15.

Photo 7.12 Ohito Viaduct

Photo 7.13 Lead Rubber Bearings, Ohito Viaduct

Photo 7.14 Unseating Prevention Device

Photo 7.15 Ohito Viaduct

b) Design

The viaduct was design in accordance with the 1985 Design Specifications of Highway Bridges (Japan Road Association). Since the seismic isolation was not yet included in the 1985 Design Specifications, the design unique in seismic isolation was referred to the Guideline for Seismic Isolation of Highway Bridges (Technology Research Center for National Land Development 1989). Both the function-evaluation and the safety-evaluation ground motions by Eqs. (6.6) and (6.7) were used in accordance with the Guideline. However the safety-evaluation ground motion by Eq. (6.8) was not use in design, since it was put in use after the 19995 Kobe Earthquake.

The natural period was set 1.32s under the safety-evaluation ground motion, which was 2.55 times the natural period of a fixed-based bridge (0.52s). This was based on the requirement in the Guideline that the natural period of an isolation bridge should be about twice the natural period of a fixed-base bridge. It resulted in the natural period of 0.73s under the function-evaluation ground motion. The natural period of 1.32s was also appropriate from a requirement that the internal force resulting from the thermal movement should be less than the seismic lateral force under the function-evaluation ground motion.

The target design displacement of a device u_B by Eq. (7.12) was assumed 201 mm and 189 mm at the intermediate isolators and the end isolators, respectively. The coefficient t c_B was assumed to be 1.0 in the Guideline. The equivalent damping ratio ξ_B was 0.15 from Eq. (7.14). Assuming the damping ratio of the deck, piers and foundations to be 0.03, 0.05 and 0.1, respectively, from Table 6.?, the first-mode damping ratio ξ_I was 0.133 based on Eq. (2.6). Consequently, the design acceleration was 0.68g under the safety evaluation ground motion.

Reinforced concrete piers were designed for the 0.68g design acceleration. The design ductility factor μ_{Ia} by Eq. (7.10) was 4.5.

Equivalent linear elastic dynamic response analysis was conducted to verify the inelastic static analysis. The 29-span viaduct was idealized by a set of beam, column and spring model. Effect of adjacent viaduct was taken into account by adding a part of the adjacent deck with the equivalent natural period and mass. A bilinear model and an equivalent linearized model idealized hysteretic behavior of isolators and piers, respectively. The soil-structure interaction effect was idealized by a set of linear soil springs. Spectral fitted ground motions were applied to the model. Table 7.2 compares the typical peak responses by the dynamic response analysis as well as the design values used in the inelastic static analysis.

Table 7.2 Peak Responses by Dynamic Response Analysis and Design Values in the Inelastic Static Analysis under Safety-Evaluation Ground Motion in Longitudinal Direction

<table>
<tr><th colspan="2">Response</th><th>Dynamic Response Analysis</th><th>Inelastic Static Analysis</th></tr>
<tr><td colspan="2">Deck Displacement</td><td>0.281m</td><td>0.328m</td></tr>
<tr><td rowspan="3">Displacement at Pier Top</td><td>P6</td><td>0.021m</td><td rowspan="3">0.026m</td></tr>
<tr><td>P14</td><td>0.022m</td></tr>
<tr><td>P29</td><td>0.017m</td></tr>
<tr><td rowspan="3">Relative Displacement of LRB</td><td>P6</td><td>0.261m</td><td>0.304m</td></tr>
<tr><td>P14</td><td>0.260m</td><td>0.285m</td></tr>
<tr><td>P29</td><td>0.265m</td><td>0.302m</td></tr>
<tr><td colspan="2">Deck Acceleration</td><td>5.77m/s^2</td><td>-</td></tr>
<tr><td rowspan="3">Bending Moment at Pier Bottom</td><td>P6</td><td>24.93MNm</td><td>30.7MNm</td></tr>
<tr><td>P14</td><td>24.2MNm</td><td>27.7MNm</td></tr>
<tr><td>P29</td><td>27.9MNm</td><td>41.5MNm</td></tr>
</table>

c) Detailings

Since the expected deck displacement resulting from the creep and shrinkage of concrete was about 130mm, repositioning of bearing after the initial setting was required. Consequently, a device was provided between a lower plate of LRB and a base plate as shown in Photo 7.16 so that flat jacks can reposition the lower plate of LRB. A special coating was provided between the two plates. After the construction was completed in October 1997, the first repositioning of 80mm was conducted in December 1997. The last positioning of 60mm is scheduled in 2004 so that the displacement of LRB resulting from the creep and shrinkage of concrete is eliminated.

Photo 7.16 Repositioning of Lower Plate, Ohito Viaduct

2) Application of High Performance Stopper and Buffer System

a) Wakayama Viaduct

Wakayama bypath, Ministry of Land, Infrastructure and Transport is a 301.5m long 12-span continuous hollow reinforced concrete slab bridge supported by 8.3-8.6m tall reinforced concrete piers as shown in Fig.7.5. A new isolator and buffer system was used in the viaduct. In the elastomeric-type isolations such as the lead rubber bearings and the high-damping rubber bearings, the laminated rubber resists the seismic lateral force under the vertical load resulting from the dead weight of a superstructure and the traffic load. Although it is beneficial in those devices to be compact, thickness of the laminated rubber that is required to accommodate relative displacement as a consequence of the seismic, thermal, creep and shrinkage effects increases as the total deck length increases.

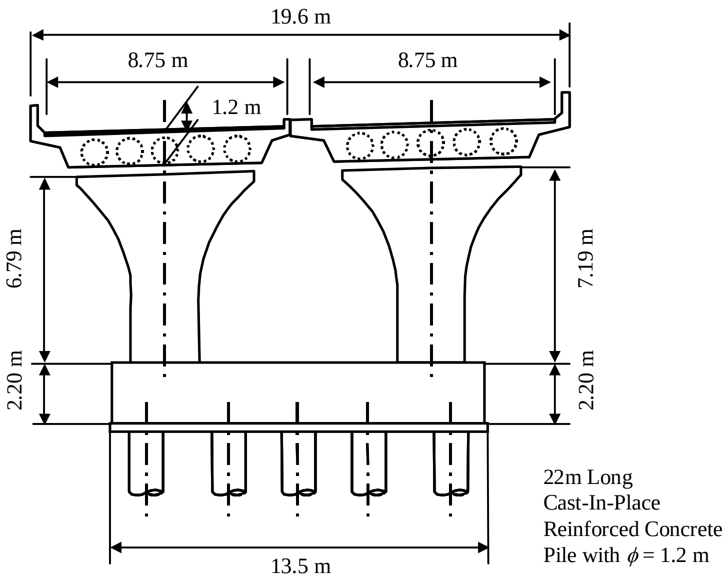

Fig.7.5 Wakayama Bypath

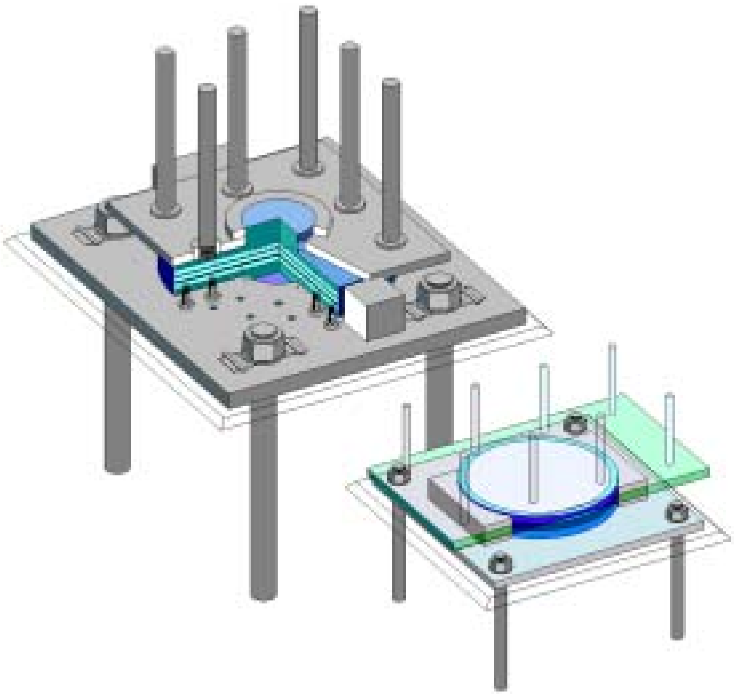

(a) Buffer (b) PTFE Sliding Bearing

Fig. 7.6 Sliding Bearing and Buffer System (Courtesy of BBM)

Consequently, a combination of high-pressure PTFE sliding bearings and laminated rubber buffers as shown in Fig. 7.6 is increasingly used in seismic isolation of long multi-span continuous bridges. This is called “high performance stopper and buffer system (HSB system).” Use of PTFE sliding bearings brings a benefit that the bearings are thinner than the normal elastomeric bearings. Since the buffers are free from the support of the dead weight of a deck, the natural period is more easily controlled than is the case with the normal elastomeric-type isolators. Consequently the system is beneficial for viaducts that sustain larger relative displacement resulting from the seismic, thermal, creep and shrinkage effects.

Since the total deck weight was 38MN, the reaction force resulting from the dead load of a deck was in the range of 4.4-5.5MN per pier in the intermediate piers. Consequently, two PTFE

Photo 7.17 Wakayama Bypath Viaduct

Photo 7.18 Sliding Bearing and Buffer System, Wakayama Bypath Viaduct

Photo 7.19 Wakayama Bypath Viaduct (Anticipated after Completed, Courtesy of Chuo Fukken Consultants)

bearings with 4MN capacity each were provided per pier. Two buffers with thickness of 112mm and size of 1160mm x 1160mm were set per pier. The shear stiffness of buffers per pier was about 13.7 kN/mm.

Photos 7.17, 7.18 and 7.19 show Wakayama Bypath that uses the HSB system. The deck was supported by two PTFE sliding bearings per pier. Two elastomeric buffers were installed per pier between a reinforced concrete block connected to the deck and two reinforced concrete blocks connected to the pier.

b) Design

Wakayama Bypath was designed in accordance with the 1996 Seismic Design Specifications of Highway Bridges (Japan Road Association 1996). The fundamental natural period was set 1.41

s. As a consequence, the design response acceleration for equivalent static analysis for the Type-II safety evaluation ground motion was 1.48g from Eq. (6.?). Since the column design ductility factor μ_{Ia} evaluated by Eq. (7.10) was larger than 8 assuming the safety factor α of 1.5 from Table 6.?, it was assumed to be 8. Consequently, the response modification factor R_μ by Eq. (7.9) was 3.8. The response modification factor R_E was assumed 1.0 in this bridge (Niwa 2000). This was because distribution of lateral force of a deck to substructures was the main concern in this bridge rather than seismic isolation. It resulted in the design response acceleration to be considered in the inelastic static analysis of 0.39g.

The buffers were designed so that shear deformation resulting from seismic effect, thermal effect and shrinkage and creep effect of concrete should not be larger than 250%. The shear deformation obtained from the inelastic static analysis was 249mm under the Type-II safety evaluation ground motion. Consequently assuming the shear deformation as a consequence of the thermal, shrinkage and creep effects to be 15mm, the thickness of buffers was determined to be 112mm. The size was determined so that shear stiffness required was obtained.

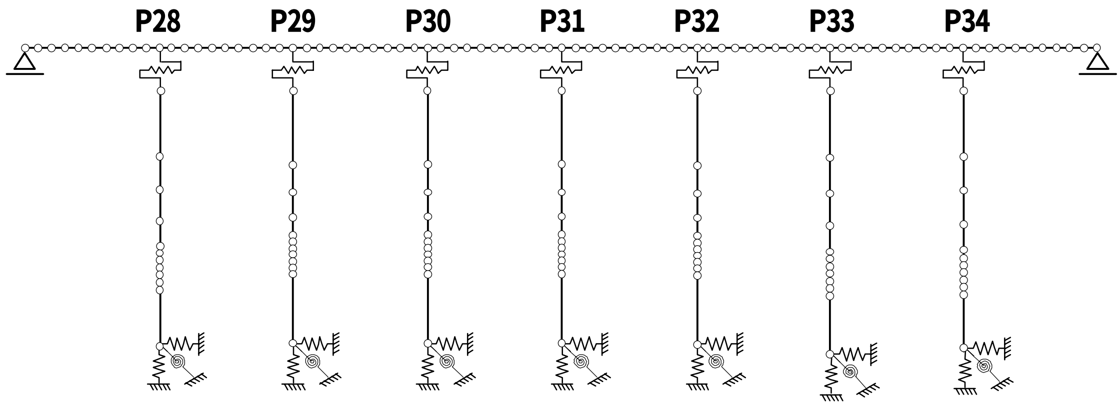

Fig.7.7 Analytical Model of Wakayama Viaduct

Nonlinear dynamic response analysis was conducted to verify the inelastic static analysis. An analytical model as shown in Fig. 7.7 was used. Hysteretic behavior of the piers was idealized by the degrading trilinear model (Takeda, Sozen and Nielsen 1970). A spectral-fitted ground motion was applied to the model. From Table 6.?, the damping ratio ξ_k of the deck, the piers, the bearings and the foundations was assumed to be 0.03, 0.02, 0.02 and 0.2, respectively. It resulted in the first mode damping ratio of the bridge ξ of 0.02. The NS component of the JMA Kobe Observatory was used an input ground motion.

Fig. 7.8 shows the response at the deck and the pier-top at center of the viaduct as well as the moment vs. curvature hysteresis at the plastic hinge of the center pier. The effect of increase of the natural period is obvious. The pier exhibits the flexural plastic behavior with the maximum moment curvature ductility factor of 3.30.

c) Cost Reduction

After the Kobe Earthquake, elastomeric bearings have been extensively adopted in bridges. This has increased the cost of bearings. In a bridge supported by steel bearings, the cost of steel bearings was only 2% in the total construction cost as shown in Fig. 7.9. However it has increased to 14.5% in a bridge supported by elastomeric bearings. It is thus effective to decrease the cost of elastomeric bearings. By adopting the HSB system, the cost of bearings decreased by 31.1% from the original design using elastomeric bearings in Wakayama Bypath Viaduct (Niwa 2000). It resulted in 6.2% cost reduction for a superstructure and bearings.

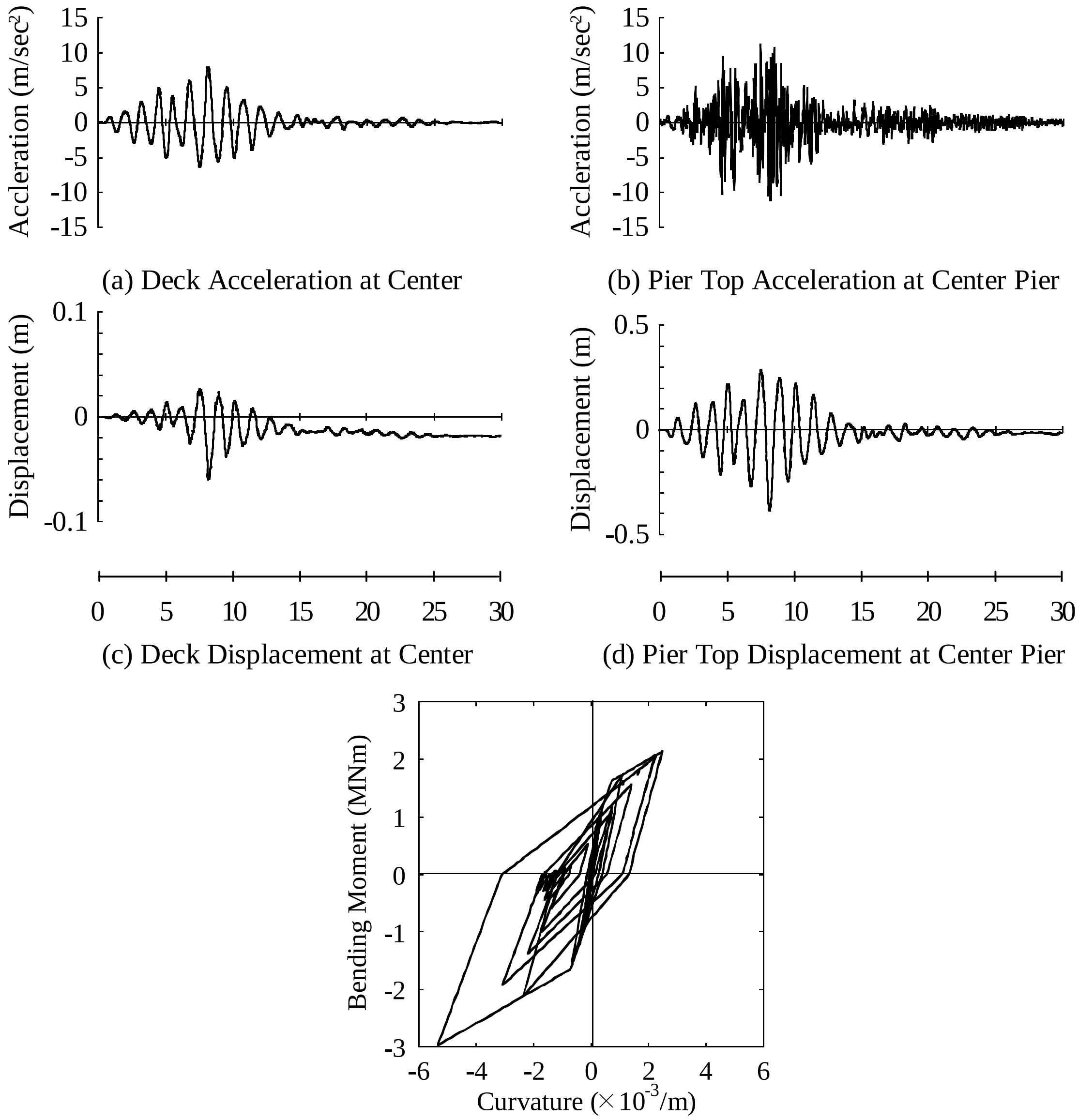

(a) Deck Acceleration at Center

(b) Pier Top Acceleration at Center Pier

(c) Deck Displacement at Center

(d) Pier Top Displacement at Center Pier

(e) Moment vs. Curvature Hysteresis at the Plastic Hinge of the Center Pier

Fig.7.8 Response Acceleration and Displacement at the Center of the Viaduct

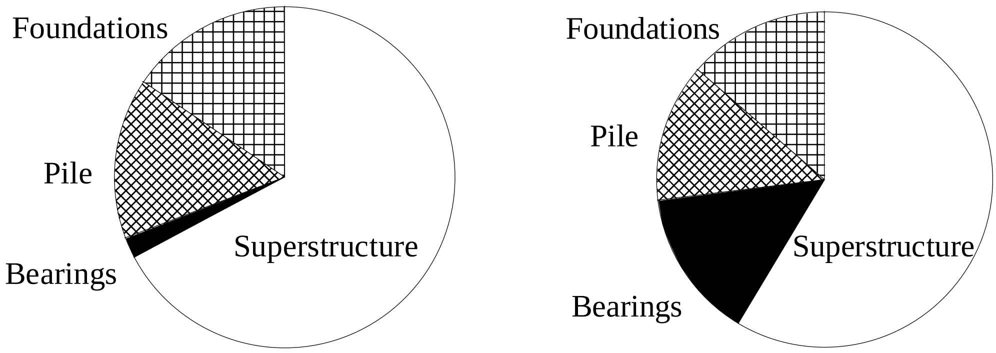

(a) Practice prior to the 1995 Hyogo-ken Nanbu Earthquake

(b) Practice after the 1995 Hyogo-ken Nanbu Earthquake

Fig.7.9 Cost Evaluation (After Niwa 2000)

3) Application to Reconstruction of a 19-span Continuous Viaduct

a) Benten Viaduct

A 20-span steel composite girder bridge at Fukae, Route 3, Hanshin Expressway, collapsed as shown in Photo 7.20 in the 1995 Kobe Earthquake. It was of six 3-span continuous and a 2-span continuous girder bridges. The damage occurred resulting from premature shear failure of reinforced concrete piers (Hayashi et al 1997, Kawashima and Unjoh 1997, Kawashima 2000b). After the earthquake, the damaged superstructure and the 21 piers were demolished. Since the pile foundations suffered minor damage, a design strategy that enabled

Photo 7.20 Collapse of Benten Viaduc, Route 3, Hanshin Expressway, in the 1995 Hyogo-ken Nanbu Earthquake

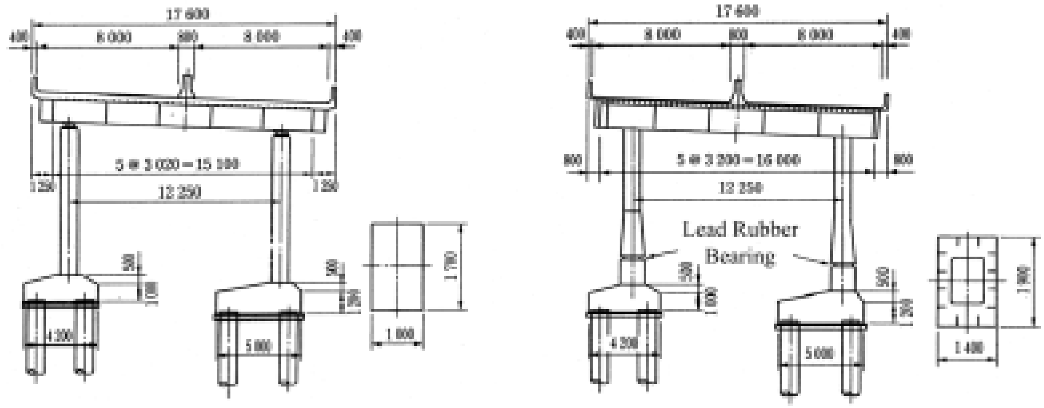

(a) Original Structure Damaged (b) Reconstructed Structure

Fig.7.10 Moment Resisting Steel Frame Pier and Steel Deck for Reconstruction of Benten Viaduct (After Hayashi et al 1997)

to re-use the foundations was sought for minimizing the reconstruction period. Consequently it was decided to construct a 19-span continuous steel box girder bridges using 20 of the 21 existing pile foundations (Hanshin Expressway Public Corporation 1997, Hayashi et al 1997).

Seismic isolation was adopted to reduce the lateral force so that the existing foundations were re-used. A unique point in the application of seismic isolation was that the lead rubber bearings were placed between the bottoms of moment resisting steel frame piers and the pedestal as shown in Fig. 7.10. Photo 7.21 shows an installation of a moment resisting steel frame. Photos 7.22 and 7.23 show a base of the moment resisting steel frame pier and a lead rubber bearing installed on a pedestal. It led to the decrease of bending moment in the pile foundations. For the same purpose, steel decks replaced the original reinforced concrete decks. Photos 7.24 and 7.25 show the Benten Viaduct after the reconstruction.

Photo 21 Moment Resisting Steel Frame Pier and Steel Deck adopted for Reconstruction of Benten Viaduct

Photo 7.22 Base of the Steel Moment Frame

Photo 7.23 Lead Rubber Bearings Installed

Photo 7.24 Benten Viaduct after Reconstruction

Photo 7.24 Benten Viaduct after Reconstruction

b) Design

Guide Specifications for Reconstruction and Repair of Highway Bridges Which suffered Damage in the Kobe Earthquake (Ministry of Construction 1995) and Menshin Manual for Highway Bridges (Public Works Research Institute 1992) were referred to in the reconstruction. Although extensive analyses were conducted, type selection and sizing were conducted based mostly on dynamic response analysis (Hayashi et al 1997). The 18-span viaduct was idealized by a discrete analytical model. Linear models with the equivalent stiffness idealized the hysteretic behavior of the steel piers and the lead rubber bearings. Application of the equivalent stiffness idealization was verified by comparing the results with inelastic dynamic response analyses. The fundamental natural period was 1.52s.

Ground motions recorded at JR Takatri Station in the 1995 Kobe Earthquake were applied to the model. Soil condition at the site was similar to that at JR Takatori Station. Damping ratio was assumed 0.02 for the deck and the piers, and 0.125 for the lead rubber bearings.

The peak response displacement of the isolators computed was 427 mm and 568 mm in the longitudinal and transverse direction, respectively. Rotation as large as 5.2 mrad and 7 mrad was predicted to occur in the isolators in longitudinal and transverse directions, respectively, resulting from rocking response of the steel piers. Lateral displacement of the isolators in longitudinal direction in the consequence of the thermal movement was 168 mm at the end of deck. Consequently a target displacement was set about 600 mm in design of the isolators.
A series of cyclic and hybrid loading test was conducted to clarify the effect of varying axial loading and rotation with us of one third model of the lead rubber bearings. It was found that the varying axial load and the rotation response do not result in important change of lateral and vertical capacity and hysteretic behavior of the isolators (Hanshin Expressway Public Corporation 1997).

7.6 Technical Development for Seismic Isolation

1) Evaluation of Seismic Response Based on a Measured Acceleration

Because of the short history of application of seismic isolation, the verification of structural performance of isolate bridges in extreme earthquakes is insufficient worldwide. Hence it is important to accumulate the measured data of seismic response of isolated bridges subjected to strong excitation. At Matsuno-hama bridge, Hanshin Expressway, a set of strong motion record as high as 0.36g was measured in the 1995 Hyogo-ken Nanbu Earthquake. It was a 211.5m long 4-span continuous steel box girder bridge supported by the lead rubber bearings at three intermediate piers and sliding bearings at two end piers as shown in Fig. 7.10. Two 103mm x 83mm lead-rubber bearings were put together in one set of bearing, and two sets were used per pier. Total thickness of the rubber was 6@21mm=126mm. It was designed based on the 1980 Design Specifications of Highway Bridges (Japan Road Association 1980), and subsequently the 1989 Guideline for Seismic Isolation of Highway Bridges (Technology Research Center for National Land Development 1989) was referred. Therefore, it was not a complete isolated bridge but a bridge that was supported by the lead rubber bearings. The response modification factor $R\mu$ was thus set 1.0 in Eq. (9). It was about 20km apart from the fault. Since ground motion was not extreme, the bridge suffered no damage.

Fig. 7.11 shows the accelerations recorded at the second pier from the right and nearby deck and ground. Acceleration sensor at the deck was provided only in longitudinal direction. It is interesting to note that the amplification of the deck acceleration relative to the pier-top acceleration was less significant, and that the period shift of the deck acceleration occurred. High acceleration in transverse direction at the pier-top was resulted from a single spike. Table 7.3 shows the peak accelerations and peak displacements.

Table 7.3 Peak Accelerations and Peak Displacements

Locations	Accelerations (g)			Displacements (mm)		
	Longitudinal	Transverse	Vertical	Longitudinal	Transverse	Vertical
Deck	0.193	-	-	24	-	-
Pier-Top	0.205	0.364	0.078	14	13	3
Footing	0.107	0.129	0.070	12	13	3
Ground	0.148	0.138	0.118	14	14	3

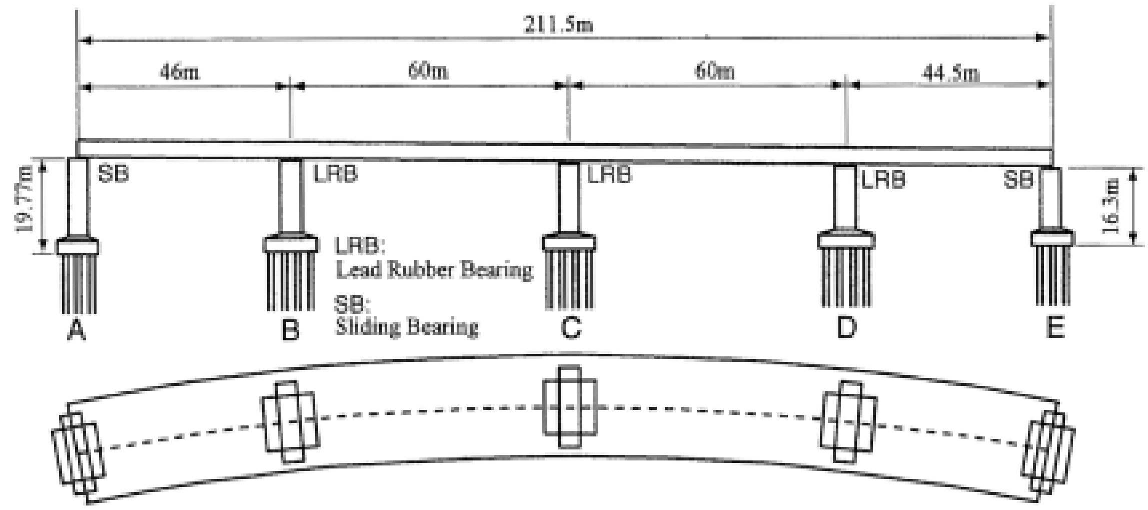

Fig. 7.11 Matsunohama Bridge, Hanshin Expressway

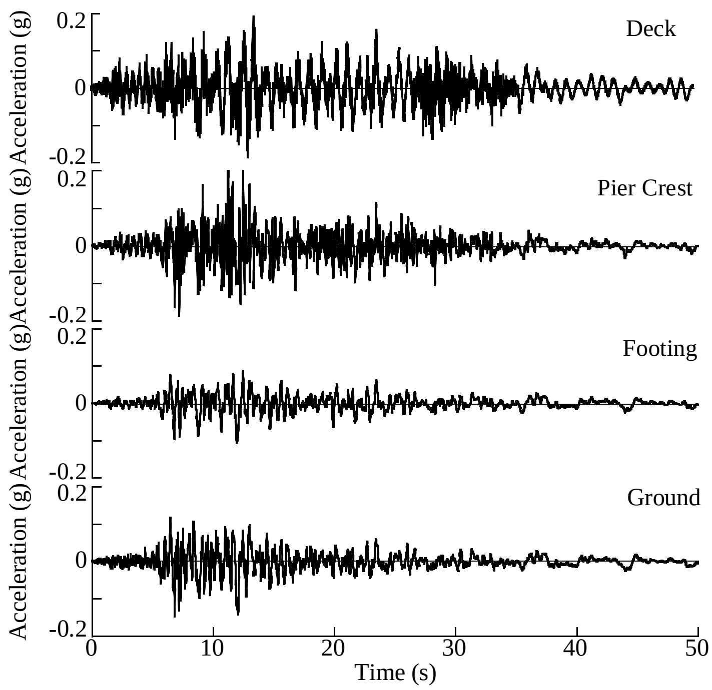

(a) Longitudinal Responses

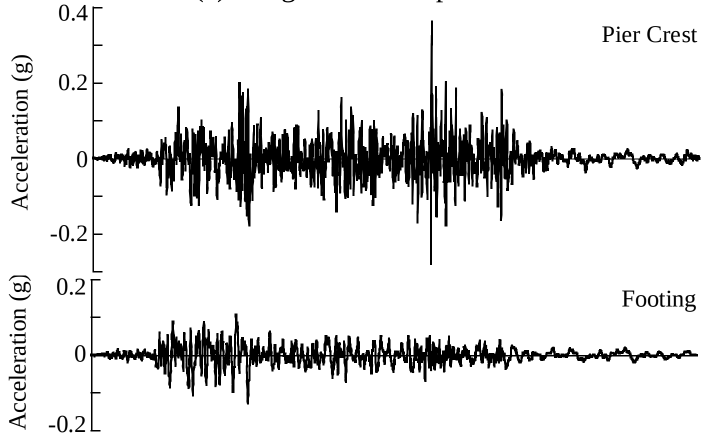

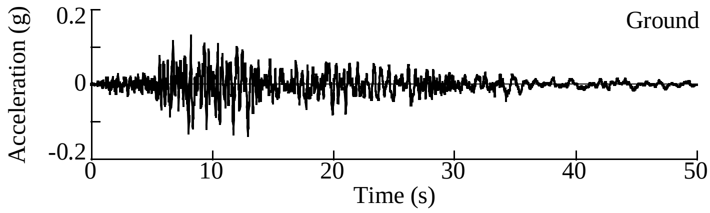

(b) Transverse Responses

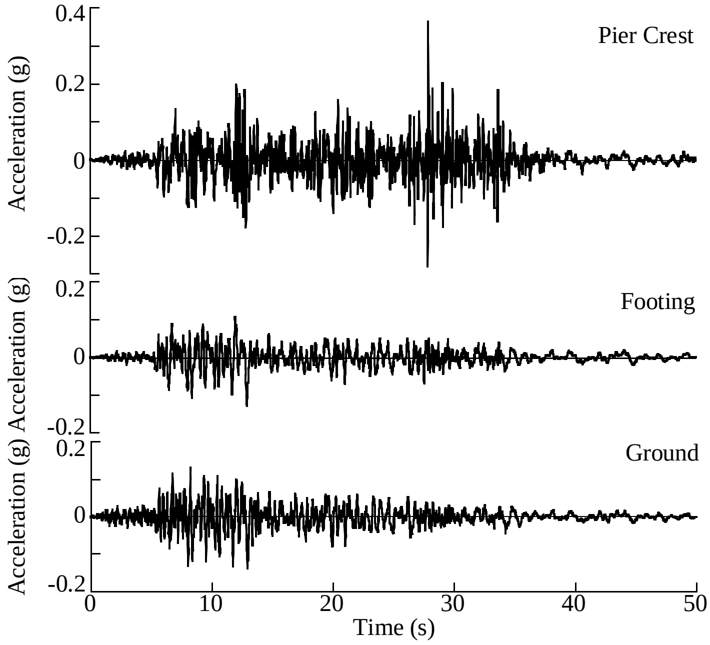

(c) Vertical Responses

Fig.7.12 Measured Accelerations at Matsunohama Bridge

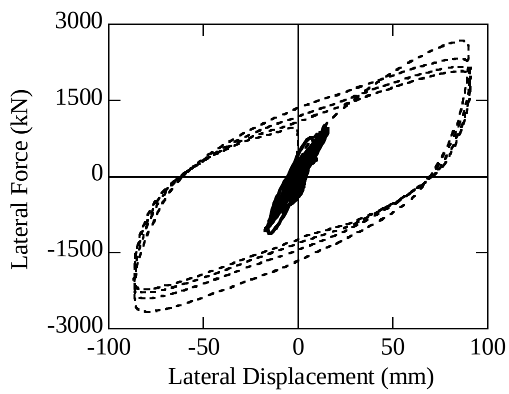

Fig.7.13 Hysteresis Estimated from the Measured Responses

Fig. 7.13 shows the lateral force vs. lateral displacement hysteresis per 2-sets bearing on a pier that was computed from the measured accelerations based on several assumptions. The lateral force vs. lateral displacement relation that was obtained in the verification test before setting in place is also presented here for comparison. The lateral displacement that occurred in the earthquake was about 16mm (about 13% shear by Eq. (20)), and was much smaller than the displacement in the verification test. Hence, the hysteresis estimated from the measured data was around the initial stiffness of the lateral force vs. lateral displacement relation obtained in the verification test.

An analytical simulation by nonlinear dynamic response analysis was conducted. A bilinear model that was used in the original design idealized the hysteretic behavior of the lead rubber bearings. Since ground acceleration was measured only at a pier, it was assumed that all foundations were subjected to the same acceleration. Fig. 7.14 shows the computed deck and pier-top accelerations in longitudinal direction. Global behavior may be represented by analysis, however more improvement of accuracy is required.

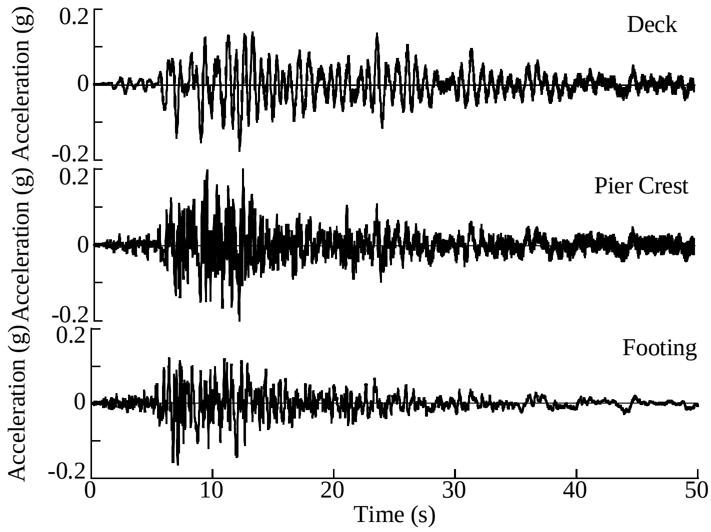

Fig.7.14 Computed Acceleration at Matsunohama Bridge

2) Development of Expansion Joints with Large Relative Displacement

It is crucial not to interrupt traffic in urban areas even after a design earthquake. Expansion joint may be a weak point in an isolated bridge where large relative displacement occurs between decks or between a deck and an abutment. As mentioned earlier, the relative displacement anticipated at an expansion joint in a standard bridge under a design ground motion reaches 0.5-0.8m, while the standard clearance between decks is 0.1-0.2m. The knock-off abutment has been implemented in New Zealand, however a half-size experimental verification using a large shaking table revealed that under such a large deck displacement, penetration of a knock-off in the back-fill side did not easily take place as shown in Photo 7.25 because a thick pavement on the back-fill resisted the motion (Kikuchi and Goto 1992).

Photo 7.25 Buckling of Asphalt Pavement on the Backfill behind a Knock-off Abutment

Two new expansion joint systems were developed. First is a sliding-type expansion joint as shown in Fig 7.15 (Unjoh, Kondo and Okahara 1999). Two sliding plates are provided at the end of adjacent decks, under an expansion joint and asphalt pavement. The sliding plates are connected to the decks by anchor bolts so that they support traffic load. The gap between two sliding plates may be 0.1-0.3m. When a relative displacement between two decks exceeds the initial gap, the anchor bolts are ruptured followed by penetration of the sliding plates into the asphalt pavement. A sharp wedge is required at the end of sliding plates so that the sliding plates easily penetrate. It may be effective to provide a Teflon sheet and a rubber sheet between the lower surface of sliding plates and the upper surface of the decks. It is called "displacement absorption joint (DAJ) system."

A series of cyclic loading tests was conducted to study the performance of the DAJ system. A 1m wide proto-type model with 50mm thick sliding plates was subjected to cyclic loading at one end with the other end being fixed. In the loading test, how to prevent buckling of asphalt pavement that was likely to occur was most important. The rubber sheet and the Teflon sheet have to be properly provided and the edge shape of sliding plates has to be properly selected.

The DAJ system was first implemented at Amano viaduct, Maibaya Bypath, a part of the National Highway 8. It is a 1.2km long 45-span viaduct. They were separated into 5 segments. The longest viaduct was of 423m long and 17-span continuous prestressed concrete hollow slabs. Since relative displacement of about +/-0.6m was anticipated at an expansion joint between decks, the DAJ system was designed so that it accommodates a relative displacement of +/-0.6m. It should be noted that the gap between two sliding plates was 40-60mm. Photo 7.26 shows the sliding plates provided.

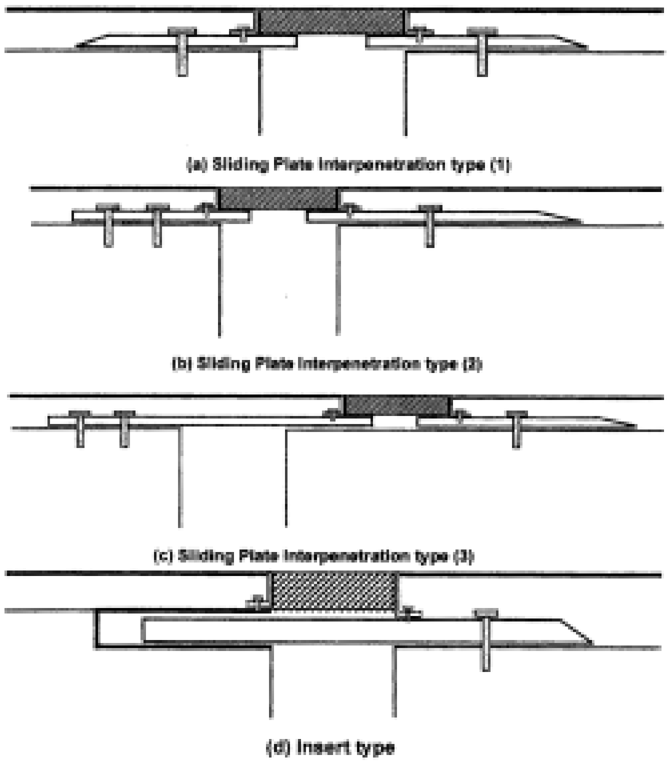

Fig. 7.15 Sliding-Expansion Joint

Photo 7.26 Sliding Plate in the Displacement Absorbing Joint

The second is an expansion joint that accommodates large relative displacement and has a function of unseating prevention device. It is called “big joint.” Since unseating prevention devices are required as well as an expansion joint, isolators and dampers at the end of deck, it is generally very busy, which makes the maintenance difficult. A new expansion joint consists of rubber cells, and longitudinal and transverse beams as shown in Fig. 7.16. Rubber cells are galvanized to the lateral beams, which slide on the longitudinal beams. By increasing the number of rubber cells, the relative displacement accommodated by the expansion joint increases as large as 0.5m in a standard bridge. The longitudinal beams have to be strong enough to support the lateral beams. Consequently, the longitudinal beams are used as an unseating prevention device for both compression and tension between two decks. Two lateral beams at the ends (end lateral beams) are anchored to decks by anchor bolts so that the lateral force can be transferred. Cyclic and hybrid loading tests were conducted for a 0.6m wide proto-type big joint to verify the performance as shown in Photo 7.27.

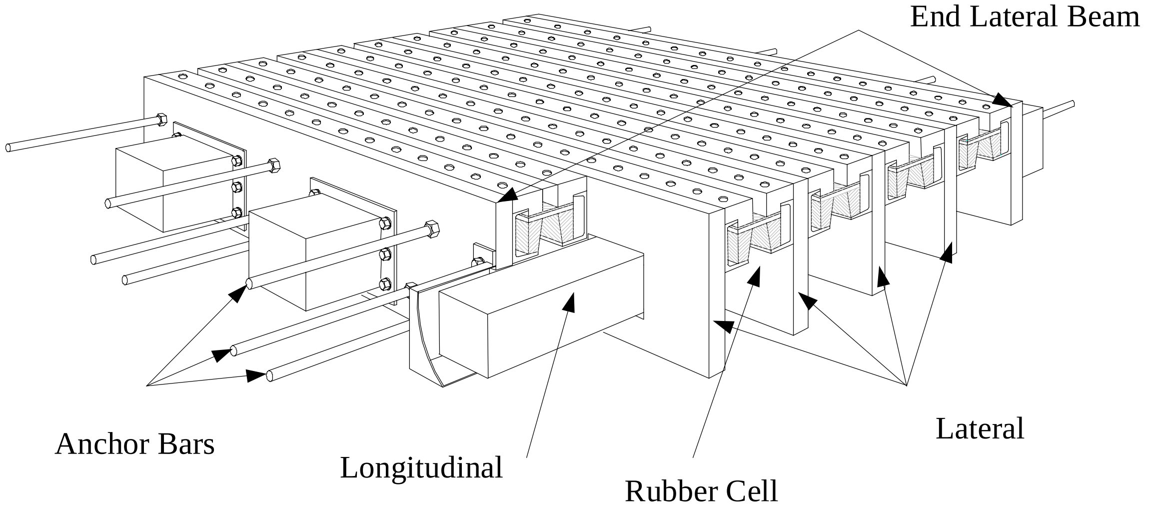

Fig.7.16 Expansion Joint with a Function of Unseating Prevention Device

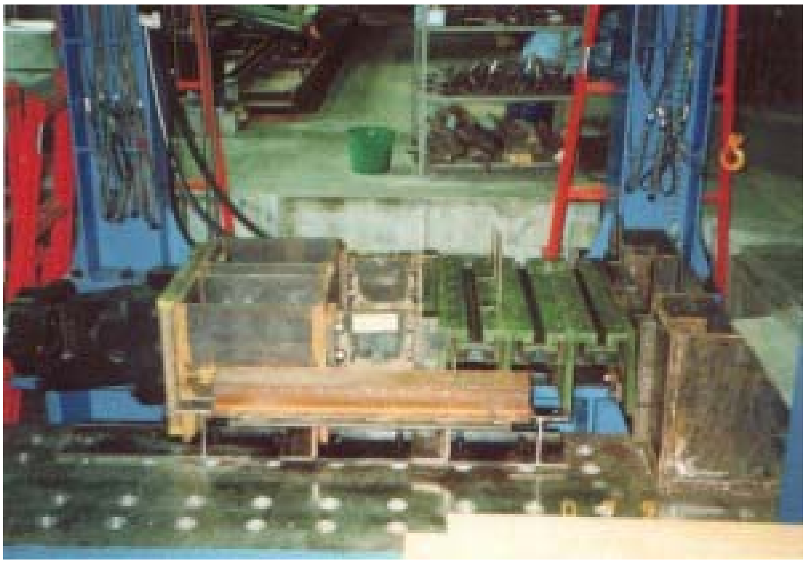

Photo 7.27 Hybrid Loading Test for a 0.6m-Wide Prototype Big Joint

3) Shock Absorbers for Mitigation of Pounding Effect

Since extensive poundings are anticipated at expansion joints to occur in an isolated bridge, it is favorable to mitigate the pounding effect. Since large strain is induced in a shock absorber during poundings, the stress-strain relation is no more linear. A compression-loading test was conducted to a number of rectangular natural rubber blocks with one side being galvanized to a steel plate as shown in Fig. 7.17. They were subjected to stress as high as 150MPa. Based on the tests, a stress σ vs. strain ε relation for a rectangular shock absorber subjected to at maximum

80% compression strain is proposed as (Uruta et al. 2000)

$$\sigma(\varepsilon, h) = \{\alpha(h)\varepsilon + \beta(h)\}\sigma(\varepsilon)_{h=150mm} \tag{7.17}$$

where

$$\begin{aligned}\sigma(\varepsilon)_{h=150mm} = {} & 5.042\times10^{-3} + 2.655\times10^{-2}\varepsilon + 1.913\times10^{-3}\varepsilon^2 - 2.158\times10^{-4}\varepsilon^3 \\ & + 1.491\times10^{-5}\varepsilon^4 - 5.383\times10^{-7}\varepsilon^5 + 1.076\times10^{-8}\varepsilon^6\end{aligned} \tag{7.18}$$

$$\alpha(h) = 0.0712\cdot\exp\left(\frac{\frac{h}{150} - 0.12}{0.136}\right) \tag{7.19}$$

$$\beta(h) = 0.969 + 2.352\cdot\exp\left(\frac{\frac{h}{150} - 0.12}{0.109}\right) \tag{7.20}$$

in which $\sigma(\varepsilon)_{h=150mm}$: stress σ at strain ε for a 150mm thick rectangular shock absorber, and h: thickness (mm) of a shock absorber. Fig. 7.18 shows a stress vs. strain relation obtained by Eq. (7.18). The relation obtained by a material and geometrical nonlinear finite element analysis is also presented for comparison. Eq. (7.18) provides an accurate estimation for the stress-strain relation of a rectangular shock absorber with a length vs. width ratio less than 4.6.

Deformation of a rectangular rubber shock absorber subjected to a pounding was investigated using a special device as shown in Photo 7.28. A weight on rails was displaced to a higher position, and it was then smoothly released to collide with a concrete wall. A shock absorber was placed in front of the weight, and it is thus subjected to a pounding force. Changing the weight and the height of displaced position, the force and velocity of collisions were controlled. Shock absorbers made of a natural rubber and a high damping rubber were tested. A steel plate was galvanized at one side of a rectangular rubber block. Parameters that affect the energy dissipation and mitigation of pounding force were studied. Static loading tests were also conducted for comparison.

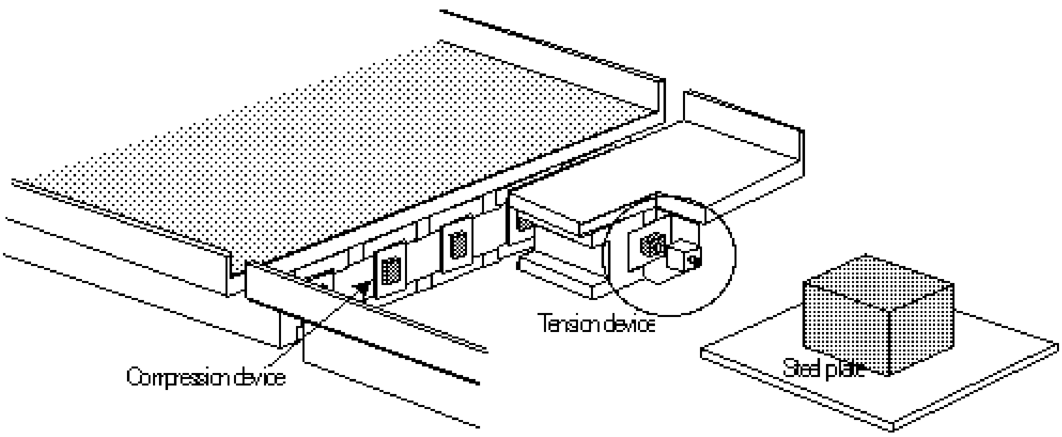

Fig.7.17 Shock Absorber

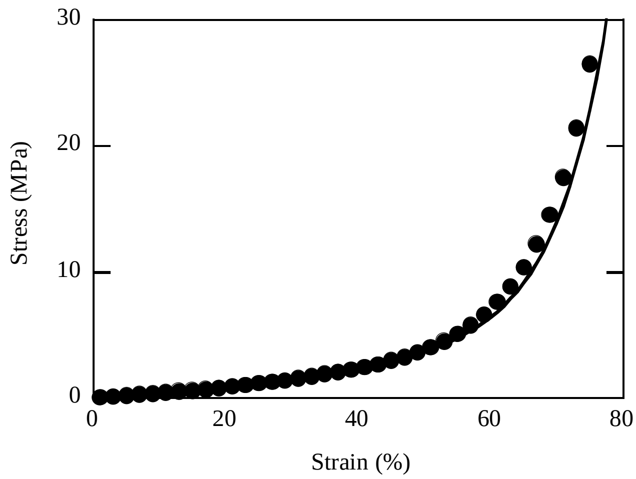

Fig.7.18 Stress vs. Strain Relation of a Shock Absorber by Eq. (21)

Photo 24 Experiment Device for Pounding Effect

Fig. 7.19 shows a comparison of the stress vs. strain relations of a natural rubber shock absorber and a high-damping rubber shock absorber between the pounding test and the static test. The loading paths are similar. Unloading paths depend on the loading velocity in the natural-rubber shock absorber, while such an effect is limited in the high-damping rubber shock absorber. Energy dissipation ratio γ is defined as

$$\gamma = \frac{\Delta E}{E_1} \tag{7.21}$$

in which ΔE : energy dissipated by a pounding and E_1: kinematic energy of a weight before pounding. Fig. 7.20 compares the energy dissipation ratio γ between the natural-rubber shock absorber and the high-damping rubber shock absorber. It is obvious that larger energy is dissipated in the high-damping rubber shock absorber.

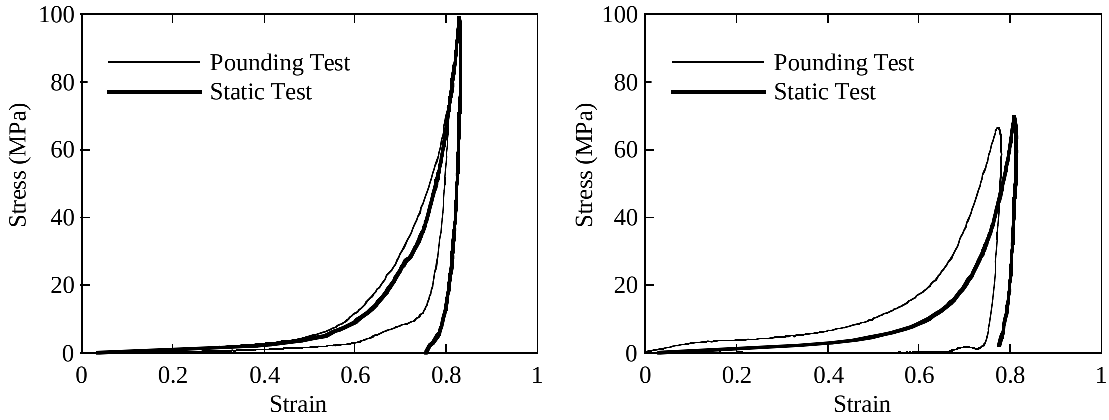

(a) Natural Rubber (b) High Damping Rubber

Fig.7.19 Comparison of Hysteretic Behavior of a Shock Absorber between Pounding Test and Static Test

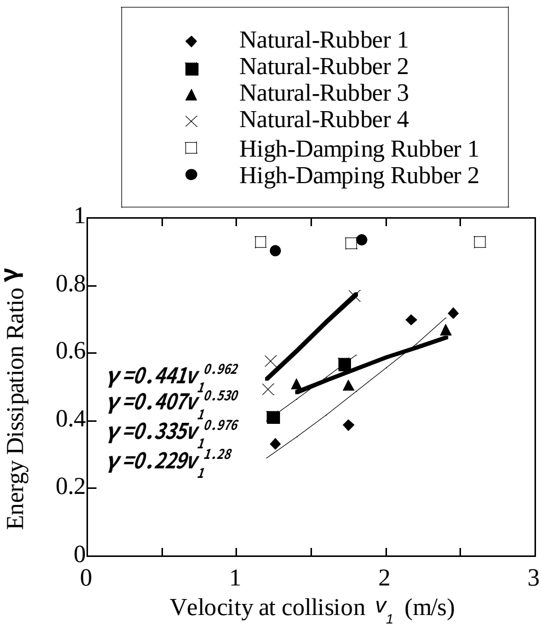

Fig.7.20 Energy Dissipation Ratio vs. Velocity of Collision

4) Effect of Pounding between Adjacent Decks

Since poundings between adjacent decks are unavoidable in an isolated bridge, this effect has to be carefully included in design. An example of analysis on the effect of the rubber shock absorber for two 200m long 5-span continuous viaducts as shown in **Fig. 7.21** is presented here (Kawashima and Shoji 2000). Since the size of elastomeric bearings is larger in the deck 2 than the deck 1, the fundamental natural period assuming the cracked-section stiffness is 0.88s and 1.13s in the deck 1 and deck 2, respectively. It was assumed that 20 100mm thick 250mm x 150mm natural-rubber shock absorbers are provided between the decks. The impact-spring idealization proposed by Tseng and Penzien (Tseng and Penzien 1973) and modified by Kawashima and Penzien (Kawashima and Penzien 1979) was used to idealize the poundings. The stiffness-degrading model (Takeda et al. 1970) was used to idealize the hysteretic behavior in the plastic hinge region of piers. Ignoring the cracking, bi-linear degrading model was assumed in analysis. The moment-curvature relation in the plastic hinge region was computed based on the standard moment-curvature analysis (Japan Road Association, 1996).

Fig. 7.22 compares response of the viaducts with and without the shock absorbers. In the bridge without the shock absorbers, pounding occurred once resulting in a large force of 146MN, 4.7 times the deck weight. This caused a pulse acceleration with 80.8g at the end of the decks. On the other hand, in the viaduct with the shock absorbers, the peak pounding force decreased to 29.6MN resulting in the decrease of deck acceleration to 3.8g. Fig. 7.23 shows the moment vs. curvature hystereses at the plastic hinge region of pier 4 at the left deck and pier 8 at right deck. The plastic flexural deformation in pier 8 decreases 22% by providing the shock absorber. It is thus obvious that shock absorbers are effective to decrease the flexural deformation of piers as well as the pounding force and deck acceleration.

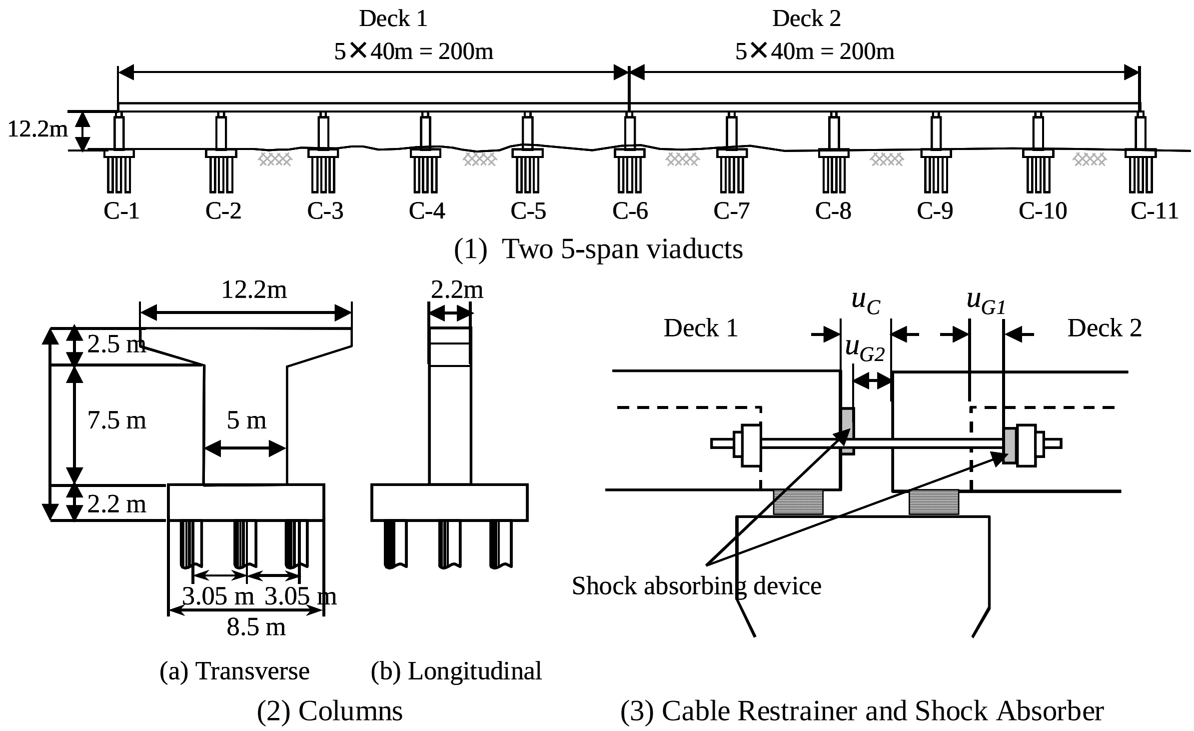

Fig.7.21 5-span Continuous Viaduct

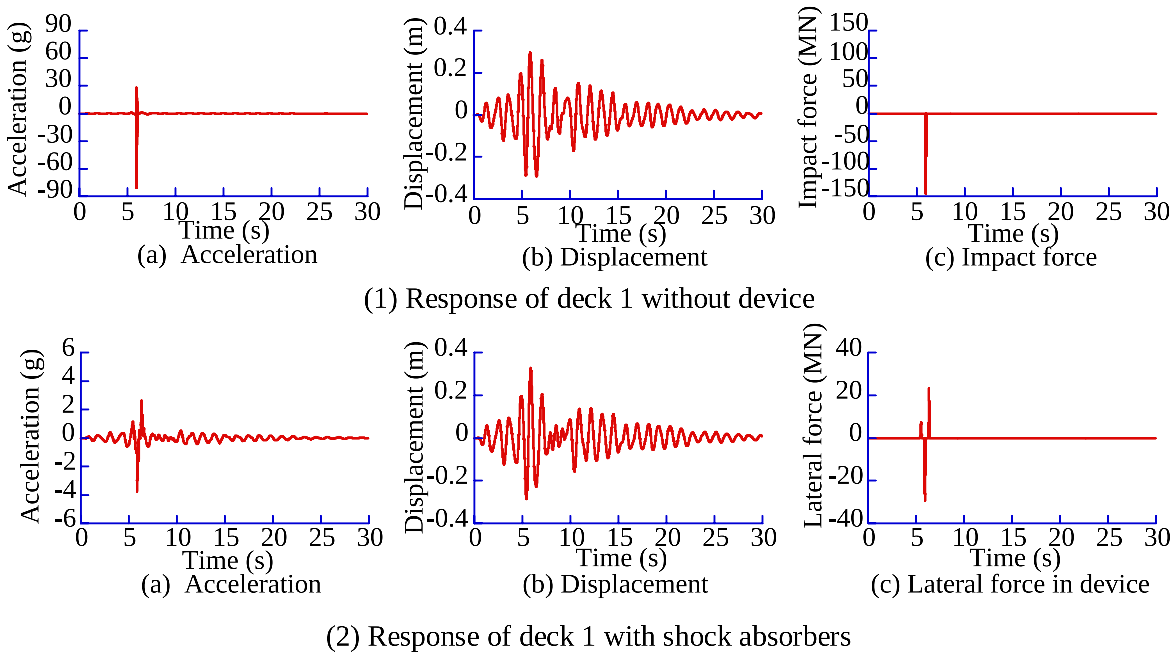

Fig.7.22 Effect of Shock Absorbers on the Deck Response

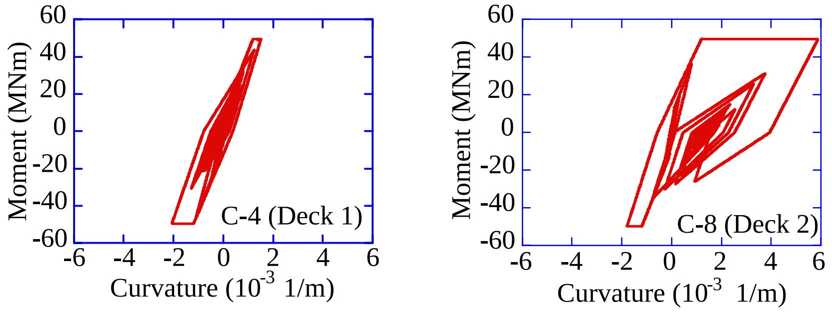

(1) Response of deck 1 and deck 2 without devices

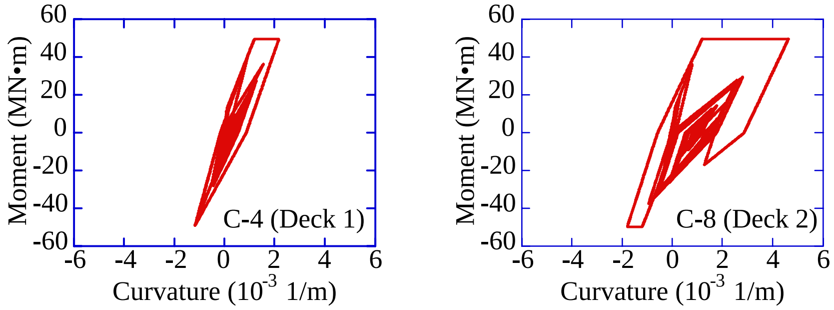

(2) Response of deck 1 and deck 2 with shock absorbers

Fig.7.23 Effect of Shock Absorbers on the Flexural Hystereses at Pier 4 and Pier 8

5) Isolator and Column Interaction

If the natural period is insufficiently increased in the Menshin Design than is the case with fixed-base condition, inelastic response of piers may be developed as well as the plastic deformation in isolators. If piers are well confined so that shear failure can be prevented, use of the Menshin Design is still beneficial no matter how some plastic flexural deformation occurs in piers. However, two points have to be clarified in such a design practice; one is the difference between the system ductility factor and system ductility factor as pointed out by Priestley et al (Priestley, Seible and Calvi 1996) in determining the response modification factor R_μ in Eq. (11). The other is the interaction of plastic deformation between isolators and piers.

When one considers a system consisting of a pier and elastomeric-type isolators such as the lead-rubber bearings and the high-damping rubber bearings, the flexural deformation of a pier and the plastic deformation of the bearings may be idealized as shown in Fig. 7.24. Representing $u_P^{\max}$ and $u_P^{P_y}$ are the peak and yield displacements of a pier, the column ductility factor μ_P may be defined as

$$\mu_P = \frac{u_P^{\max}}{u_P^{P_y}} \tag{7.22}$$

Representing the displacement of a deck resulting from the plastic flexural deformation of a pier as u_{Pp} given by

$$u_{Pp} = u_P^{P_y}(\mu_P - 1) \tag{7.23}$$

the system ductility factor μ_S may be defined as

$$\mu_S = \frac{u^{\max}}{u^{P_y}} \tag{7.24}$$

where

$$u^{P_y} = u_P^{P_y} + u_B^{P_y} \tag{7.25}$$

$$u^{\max} = u^{P_y} + u_{Pp} \tag{7.26}$$

in which u^{P_y} and $u_B^{P_y}$: displacement of a deck and bearings, respectively, developed under a lateral force equivalent to the column yield capacity P_y, and $u^{\max}$: peak deck displacement. Substituting Eqs. (7.24), (7.25) and (7.26) into Eq. (7.24), one obtains

$$\mu_S = 1 + \frac{\mu_P - 1}{1 + c_f} \tag{7.27}$$

where c_f is called bearing-flexibility factor, given as

$$c_f = \frac{u_B^{P_y}}{u_P^{P_y}} \tag{7.28}$$

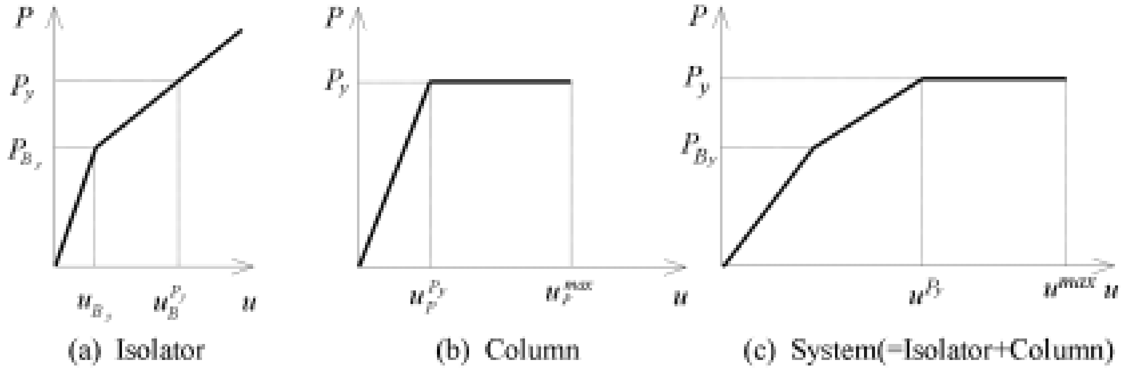

Fig.7.24 Lateral Force vs. Lateral Displacement Relation

Two viaducts were analyzed for clarifying the effect of the column ductility factor and the system ductility factor on the response modification actor $R\mu$; one is a 200m long 5-span continuous steel girder bridge, and the other is an 110m long 4-span continuous reinforced concrete hollow slab bridge. 10m tall reinforced concrete columns support both bridges. The first bridge is supported by 5 lead rubber bearings per column while the second bridge is supported by 5 high-damping rubber bearings per column. The fundamental natural period assuming the cracked-section column stiffness and design displacement of the bearings u_B is 1.24s and 408mmm in the first bridge and 1.81s and 178mm in the second bridge. The bearing-flexibility factor c_f by Eq. (7.28) is 9.0 and 24.6 in the first and the second bridges, respectively. Hence it is obvious that the system ductility factor μ_S is much smaller than the column ductility factor μ_P.

This has to be taken into account in the evaluation of response modification factor R_μ by Eq. (7.9). Response modification factors were evaluated by both Eq. (7.9) and nonlinear dynamic response analyses for many bridges. It is obvious from Fig. 7.25 that the system ductility factor μ_S should be used instead of the column ductility factor μ_P in Eq. (11) (Kawashima and

Nagai 2001).

Both cyclic and hybrid loading tests were conducted to clarify the effect of bearing flexibility on the system ductility of a pier-isolator system (Kawashima, Shoji and Saito 2000). Six 1.75-1.85m tall reinforced concrete piers with a section of 400mm x 400mm were constructed, and three 100 mm thick high-damping rubber bearings were attached on the piers by anchor bolts. Flexural capacity of the piers was varied in three levels (Type-A, B and C specimens) as shown in Fig. 7.26 with the capacity of the bearings being unchanged. Defining the yield capacity ratio ς as

$$\varsigma = \frac{P_y^B}{P_y} \tag{7.29}$$

ς is 0.61, 0.53 and 0.38 in Type-A, B and C specimens, respectively, in which P_y and P_y^B are yield capacity of a pier and a bearing, respectively. Since ς is in the range of 0.2-0.3 in a standard viaduct, the yield capacity of bearings is higher in the test than is the case in the standard condition.

The pier-bearing system was laterally loaded at the top-surface of the bearings under a constant axial load. Fig. 7.27 shows lateral force vs. lateral displacement hystereses of the pier and the bearing. Since the post-yield stiffness of bearing is positive, plastic flexural deformation eventually occurs in the piers as the loading displacement increases. The flexural deformation of the pier decreases as the yield capacity ratio ς increases. Similar to the bearing flexibility factor c_f by Eq. (7.28), a displacement-dependent bearing flexibility factor c_{fu} was defined as

$$c_{fu} = \frac{u_{B\max}}{u_{P\max}} \tag{7.30}$$

in which $u_{B\max}$ and $u_{P\max}$ are peak displacement of the bearing and the pier, respectively, during a load reversal. Fig. 7.28 how the displacement-dependent bearing flexibility factor c_{fu}. As the pier displacement increases c_{fu} decreases as a consequence of the degradation of the pier. It is thus important to use c_{fu} corresponding to the design ductility factor.

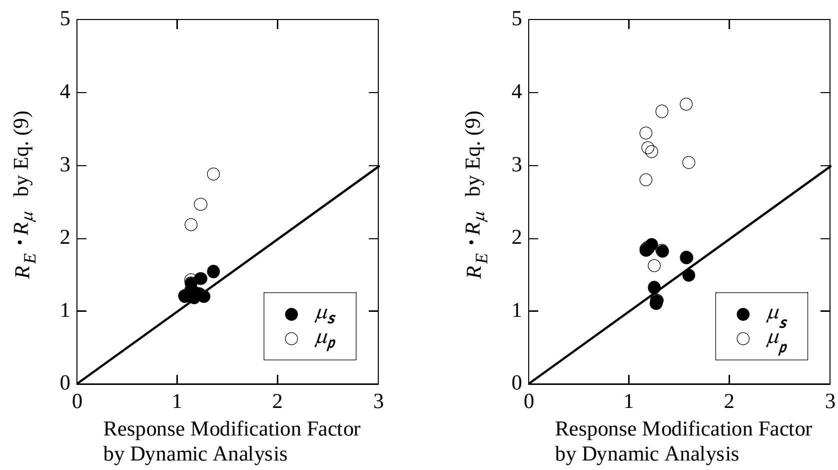

(a) Steel Girder Bridge (b) Reinforced Concrete Hollow Bridge

Fig.7.25 Dependence of Response Modification Factor on the Column Ductility Factor and the System Ductility Factor

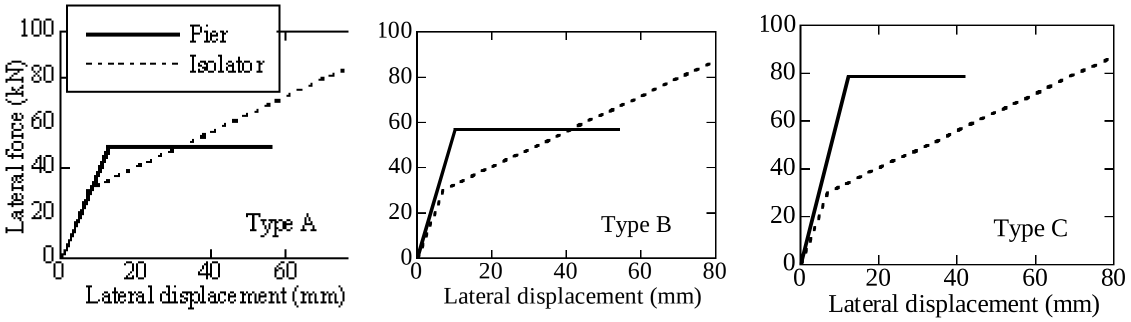

(a) Type-A (b) Type-B (c) Type-C

Fig.7.26 Lateral Force vs. Lateral Displacement Relation of a Column and an Isolator

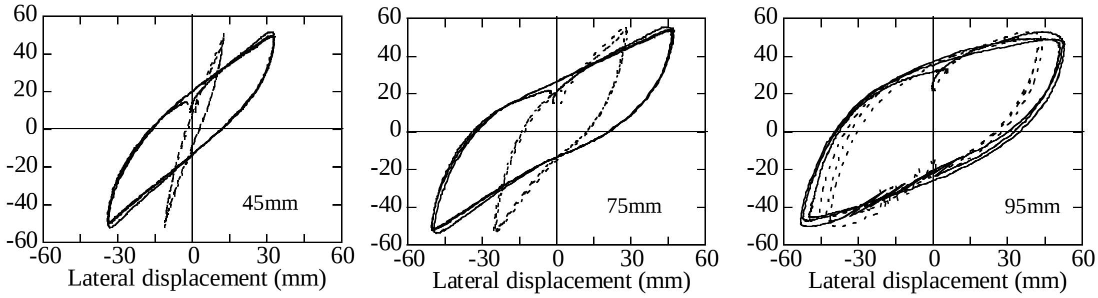

(a) Displacement= 45mm (b) Displacement=75mm (c) Displacement=95mm

Fig.7.27 Hystereses of a Column and an Isolator

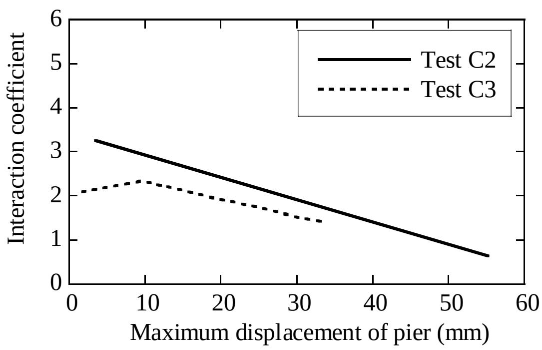

Fig.7.28 4Displacement Dependent Bearing Flexibility Factor

7.7 Active and Semi-Active Response Control

1) Active Control

2) Semi-Active control

3) Response Controlled by Variable Damper

a) Variable Dampers for Application in Bridges

A unique technology in the application of dampers to bridges is the distribution of lateral force to as many piers as possible. Although a damper is effective for reducing deck response, it is also effective for transmitting lateral force from the deck to piers when it is used in the over-damped range. Such an application of a damper may be called the "damper stopper" (Matsumura *et al* [21]). Elongation or shrinkage of the deck due to temperature change, which become predominant in multi-span continuous bridges, can be absorbed by the damper stopper, because the damper stopper does not resist relative movements with low loading rate. Thus damper stoppers have been successfully implemented in many bridges.

However, little energy dissipation occurs in the damper stoppers, because the damping ratio is set very high. It is an effective play to decrease the damping ratio to obtain greater energy dissipation when the bridge is subjected to ground motion caused by a large earthquake. Because the damper stopper is effective for preventing small deck vibration associated with braking loads and wind effects, the function of a damper stopper is effective at small deck displacement. On the other hand, when the deck response becomes excessive during an earthquake, the stopper is required to prevent further buildup of the deck response.

Thus, variable dampers with the following characteristics are superior to existing dampers and damper stoppers (Kawashima and Unjoh [14]):

(a) The damping coefficient is very large during small deck vibrations for preventing deck vibration due to braking and wind loads. The damper is movable in low-rate motions such as the thermal movement of a deck.

(b) To counteract seismic response when the deck response exceeds a certain threshold value, the damping coefficient needs to be set so as to maximize energy dissipation.

(c) To prevent excessive deck response during an earthquake, a high damping coefficient is required for the damper to function as a stopper. A smooth and gradual increase of the damping force may be effective for preventing shocks.

Thus, the variable damper has the advantages of a damper stopper, a passive energy dissipater, and a stopper with a shock absorber.

Although various types of variable dampers can be made, the simplest device may be a piston-cylinder viscous damper as shown in Fig. 7.29. A bypass is installed between the cylinder cells divided by the piston. The damping coefficient of the damper can be controlled by varying the amount of viscous flow through the bypass. The external energy required for such

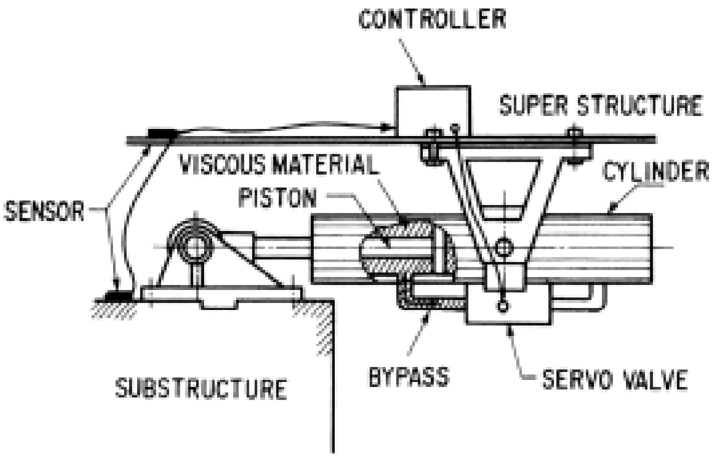

Fig. 7.29 Variable Damper

control is generally much smaller than that required for active control.

b) Analytical Model

To demonstrate the effectiveness of the variable damper, various seismic response analyses were conducted. The damping coefficient was assumed in the analysis to vary as shown in Fig. 27. The damping coefficient is C_2 at relative displacement d=0; it decreases linearly to C_1 at $d = \pm d_u / 6$, where d_u represents the maximum relative displacement developed between the deck and the pier without control; it is C_1 between $\pm d_u/6$ and $\pm 2d_u/3$; and it linearly builds up to C_3 at $d = \pm d_u$. It is possible to vary C_1, C_2 and C_3 in time depending on the bridge response to optimize the deck response, but for simplicity, they were assumed here to be constant during an earthquake.

The equations of motion for a linear multi-degree-of-freedom system with variable dampers may be written in the incremental form as

$$\mathbf{M}\Delta\ddot{\mathbf{u}}_t + (\mathbf{C}^S + \mathbf{C}_t^V)\Delta\dot{\mathbf{u}}_t + \mathbf{K}\Delta\mathbf{u}_t = -\mathbf{MB}\Delta\ddot{\mathbf{u}}_g \tag{7.31}$$

in which $\mathbf{C}^S$ = damping matrix of the system; and $\mathbf{C}_t^V$ = damping matrix representing the variable dampers. It is assumed as

$$\mathbf{C}_t^V = \sum_{k=1}^{n_V} \mathbf{c}_{tij}^V \tag{7.32}$$

where

$$\mathbf{c}_{tij}^V = \begin{bmatrix} C & -C \\ -C & C \end{bmatrix} \tag{7.33}$$

in which $\mathbf{c}_{tij}^V$ = element damping coefficient matrix of a variable damper at time t installed between i-th and j-th node; n_V = number of variable dampers; and C = damping coefficient of variable damper.

It should be noted that any relation between the damping coefficient C and the relative displacement and/or relative velocity can be incorporated in the analysis.

Assuming that the damping matrix $\mathbf{C}^S$ can be diagonalized by the modal matrix similar to Eqs. (2.25) and (2.26), the damping matrix $\mathbf{C}^S$ was given as

$$\mathbf{C}^S = (\Phi)^{-1} diag(2h_k\omega_k)(\Phi^T)^{-1} \tag{7.34}$$

in which Φ = a modal matrix of the system; $diag(2h_k\omega_k)$ = a diagonal matrix containing $2h_k\omega_k$ (k $=1,2,\cdots\cdots,n$, n; mode number); h_k = modal damping ratio for k-th mode; and ω_k = natural frequency for k-th mode.

c) Seismic Response Analysis of a Bridge with Variable Damper

To show the performance of bridges with variable dampers, a single-span bridge, as shown in Fig. 7.30, with a span length of 30 m was analyzed. Although the variable damper is better implemented in multispan continuous bridges, a single-span bridge was analyzed here for simplicity. The deck was assumed to be supported by elastomeric bearings, and two variable dampers were installed between the deck and the piers.

The seismic response of the model bridge was analyzed assuming the damping coefficient C vs. relative displacement relation of the variable damper as shown in Fig. 7.31. Case-1 represents the bridge response without the variable damper. Case-2 is for studying the most appropriate damping ratio h_1. Cases 3 and 4 are for studying the effect of a weak stopper and a strong stopper. The damping ratio h_3 was assumed as 3 in Case 3 and 500 in Case 4. Case 5 is for studying the effect of a damper stopper at small displacement.

Fig. 7.32 shows how the peak deck response and the forces developed at the bottom of piers vary by the damping ratio h_1 in Case 2. The peak deck displacement simply decreases as the damping ratio h_1 increases. The peak deck acceleration becomes minimum at a damping ratio h_1 of about 0.5. The deck acceleration increases as the damping ratio increases over 0.5, where the variable dampers function as damper stoppers rather than energy dissipaters. The bending moment and shear force at the bottom of piers, which are important for seismic design, vary in a similar manner to the deck acceleration. As the damping ratio increases, the maximum damping force developed in the variable dampers increases, while the stroke of the piston decreases. The total energy dissipated during the excitation becomes maximum at a damping

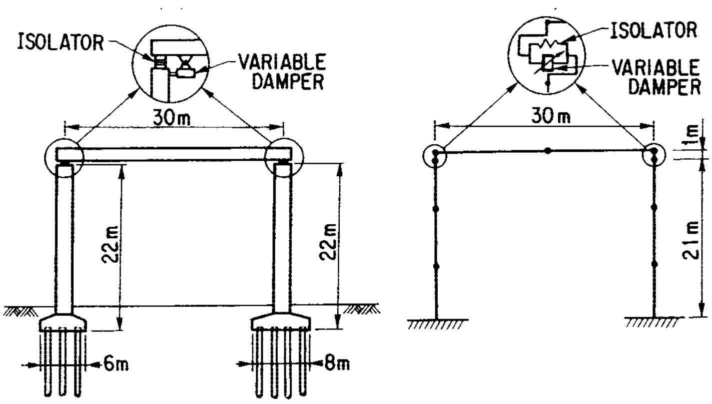

Fig. 7.30 Bridge (a) Analyzed: (b) Analytical Idealization

Fig. 7.31 Analytical Cases: (a) Case 1; (b) Case 2; (c) Case 3; (d) Case 4; (e) Case5; (f) Case 6

ratio h_1 of 0.2.

Assuming h_1 =0.5, the effect of the variable dampers for restricting excessive relative displacements was then analyzed. The relative displacement between the deck and the pier d_u was assumed as 7.67 cm, which was the peak relative displacement in Case 2. Fig. 31 compares the deck response, the forces at the bottom of piers, the damping force, the stroke, and the energy dissipated by the variable dampers. By providing variable dampers, the relative displacement of deck is reduced from 7.67 cm to 6.9 cm with the weak stopper (Case 3) and 5.54 cm with the strong stopper (Case 4). This means that the variable dampers are as effective as a damper stopper for limiting the relative displacement of the deck. This effect is more significant with the strong stopper. However, as the damping ratio h_3 increases, the damping force induced in the variable dampers increases.Fig. 7.33 shows the effect of a damper stopper at small deck displacement. The damping ratio h_1 was assumed as 0.5. As can be deduced from Fig. 30, although the deck displacement simply decreases as the damping ratio ξ_2 increases, the deck acceleration and the force at the bottom of piers become minimum at $\xi_2 = 0.5$. The damping ratio h_2 has to be determined not from the seismic response point of view but from the

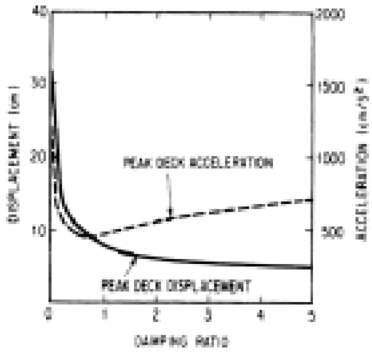

(a) Deck Response

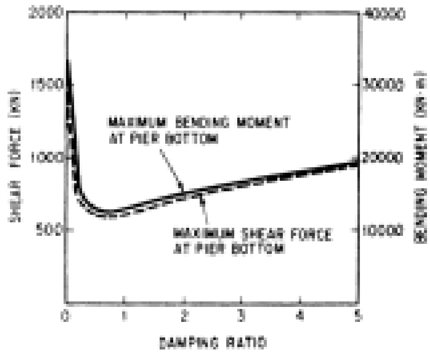

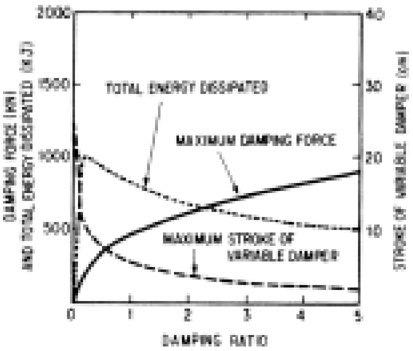

(b) Forces at Pier Bottom (c) Response of Variable Damper

Fig. 7.32 Peak Response and Damping Force Developed in Variable Dampers(Case 2

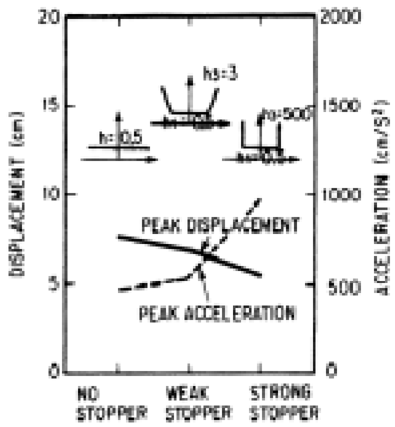

(a) Deck Response

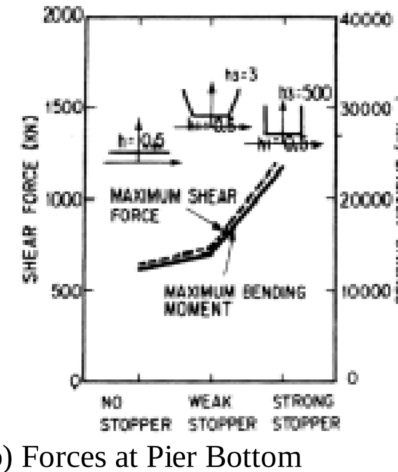

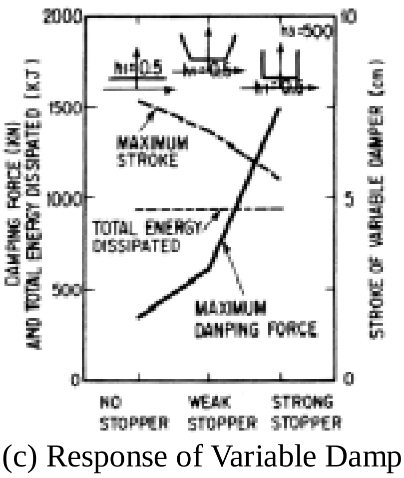

(b) Forces at Pier Bottom (c) Response of Variable Damper

Fig. 7.33 Effect of Weak Stopper (Case 3) and Strong Stopper (Case 4) requirement for stability against the braking load and wind effect. It was then assumed $\xi_2 = 3$.

Based on the results presented above, it is most appropriate to assume a damping ratio of $\xi_1 = 0.5$ and $\xi_2 = \xi_3 = 3$ (Case 6). As shown in Table 7.4, the peak deck displacement and acceleration decrease to 26 % and 44 % of those without variable damper, respectively. The maximum bending moment at the bottom of piers decreases to 47 % of that without variable damper.

The damping force and stroke required for the variable dampers are 614 kN x 2 = 1,228 kN and 5.78 cm, respectively. Because the weight of the deck is 2,368 kN, the damping force is 52 % of the deck weight. Variable dampers with this requirement can be designed and fabricated within the current technology for dampers.

Table 7.4 Peak Responses

Analytical Cases		Case 1	Case 2	Case 3	Case 4	Case 5	Case 6
Deck	Displacement (cm)	33.00	10.28	9.94	10.90	8.50	8.46
	Velocity (cm/sec)	189.0	60.2	54.2	76.4	51.3	48.4
	Acceleration (gal)	1,300	478	538	965	567	567
Pier	Shear Force(kN)	1,637	622	706	1,215	786	786
	Moment(kNm)	32,333	11,994	13,680	23,359	15,102	15,102
Variable Damper	Damping Force(kN)	-	340	590	1,484	634	614
	Stroke (cm)	-	7.67	6.90	5.54	6.34	5.78
	Velocity (cm/s)	-	44.9	68.1	112.3	55.8	60.7
	Total Energy (kJ)	-	921	926	931	731	731

REFERENCES

Buckle, I. and Mayes, R., 1992, “History and Application of Seismic Isolation to Highway Bridges”. Proc. 1st US-Japan Workshop on Earthquake Protective Systems, NCEER 92-4, pp. 27-40, National Center for Earthquake Engineering Research, State University of New York, Buffalo, NY, USA.

Enomoto, Takano, Ogasawara, Takahashi, Watanabe, Inoue, 1994, "Design and Study of the Tsurumi Fairway Bridge," IABSE, Deaville, France.

Fukuda, S., 1980, “Design of Multi-span Continuous Highway Bridges with Use of Shear-Viscous Damper,” Bridges and Foundations, Tokyo, Japan (in Japanese)

Hayashi H. Kawakita, S., Nakahigashi, T. and Sanada, K., 1997, "Design of the 19-span Continuous Rigid Frame Bridge with Seismic Isolator," IABSE Symposium on New Technologies in Structural Engineering, Lisbon, Portugal

Iseki, J., 1980, “Shear Viscous Damper-Application to Design of Multi-span Continuous Bridges, Bridges and Foundations, Tokyo, Japan (in Japanese).

Japan Road Association, 1964, 1980, 1990, 1996, “Design Specifications of Highway Bridges,” Maruzen, Tokyo, Japan

Kanemitsu, H. and Higuchi, K., 1981, “Displacement Control of Bridges with Suspended Girder, Technical Report of Honshu-Shikoku Bridge Authority, Tokyo, Japan (in Japanese)

Kato, N., Iioka, Y. and Kawahito, T., 1983, “Design of Meiko-Nishi Bridge,” Bridges and Foundations, Tokyo, Japan (in Japanese).

Kawashima, K. and Penzien, J., 1979, “Theoretical and Experimental Dynamic Behavior of a Curved Model Bridge Structure, Earthquake Engineering and Structural Dynamics,” Vol. 7, pp. 129-145.

Kawashima, K., Aizawa, K. and Takahashi, K., 1984, “Attenuation of Peak Ground Motions and Absolute Acceleration Response Spectra,” Proc. 8WCEE, Vol. II, pp. 257-264, San

Francisco, CA, USA
Kawashima, K. and Aizawa, K., 1986, "Modification of Earthquake Response Spectra with Respect to Damping Ratio," 3rd US National Conference on Earthquake Engineering, Charleston, SC, USA
Kawashima, K., 1992, "A Perspective of Menshin Design for Highway Bridges, " Proc. 1st US-Japan Workshop on Earthquake Protective Systems for Bridges, pp. 3-26, Technical Report NCEER 92-4, National Center for Earthquake Engineering Research, State University of New York, Buffalo, NY, USA
Kawashima, K., 1994, "Menshin Design of Highway Bridges in Japan," Proc. 3rd US-Japan Workshop on Earthquake Protective Systems of Bridges, Technical Report NCEER 94-9, pp. 1.3-1.31, National Center for Earthquake Engineering Research, State University of New York, Buffalo, NY, USA
Kawashima, K. and Unjoh, S., 1997, "The Damage of Highway Bridges in the 1995 Hyogo-ken Nanbu Earthquake and Its Impact on Japanese Seismic Design," Journal of Earthquake Engineering, Vol. 1, No. 3, pp. 505-541.
Kawashima, K., 2000a, "Seismic Design and Retrofit of Bridges," Key Note Presentation, 12th World Conference on Earthquake Engineering, Paper No. 1818 (CD-ROM), Auckland, New Zealand
Kawashima, K., 2000b, "Seismic Performance of RC Bridge Piers in Japan," Progress in Structural Engineering and Materials, Vol. 2, No. 1, pp. 82-91.
Kawashima, K. and Shoji, G., 2000, Effect of Restrainers to Mitigate Pounding between Adjacent Decks subjected to a Strong Ground Motion," 12th World Conference on Earthquake Engineering, Paper No. 1435 (CD-ROM), Auckland, New Zealand
Kawashima, K., Shoji, G. and Saito, A., 2000, "Column and Isolator Interaction in an Isolated Bridge," Proc. 2nd International Workshop on Mitigation of Seismic Effects on Transportation Structures, pp. 161-172, Taipei, Taiwan, R.O.C.
Kawashima, K. and Nagai, M., 2001, "Effect of Column and System Ductility Factors on the Evaluation of Response Modification Factor of Isolated Bridges," Proc. Structural and Earthquake Engineering, No. 675/I-55, pp. 235-250, Japan Society of Civil Engineers, Tokyo, Japan (in Japanese).
Kikuchi, T. and Goto, Y., 1992, "Lateral Loading Tests of Knock-off Mechanism for Menshin Bridges," Proc. 1st US-Japan Workshop on Earthquake Protective Systems of Bridges, Technical Report NCEER 92-4, pp. 221-231, National Center for Earthquake Engineering Research, State University of New York, Buffalo, NY, USA
Kitazawa, M., Iseki, J. and Shimoda, I, 1994, "Development of New Type Damper for Cable Stayed Bridge," Proc. 3rd US-Japan Workshop on Earthquake Protective Systems of Bridges, Technical Report NCEER 94-9, pp. 2-39-2-46, National Center for Earthquake Engineering Research, State University of New York, Buffalo, NY, USA
Kuribayashi, E. and Iwasaki, T., 1972, "Dynamic Properties of Highway Bridges," Proc. 5WCEE, Roma, Italy
Matsuno, H., Hara, K. and Yamashita, M., 1994, "Design Plan of Super Multi-span Continuous Menshin Bridge with Deck Length of 725m," Proc. 3rd US-Japan Workshop on Earthquake Protective Systems of Bridges, Technical Report NCEER 94-9, pp. 4-69-4-84, National Center for Earthquake Engineering Research, State University of New York, Buffalo, NY, USA
Okamoto, S. and Uemae, Y., 1963, "Aseismic Bridge Structure by Elastic Supports using Tie Members (SU-Damper), Proc. Symposium on New Ideas in Structural Design, Japan Society of Civil Engineers and Architectural Institute of Japan, Tokyo, Japan (in Japanese).
Priestley, N.M.J, Seible, F. and Calvi, G. M., 1996, "Seismic Design and Retrofit of Bridges," John Wiley & Sons, New York, US

Public Works Research Institute, 1992, “Menshin Manual of Highway Bridges” Tsukuba, Japan.

Robinson, W. H. and Greenbank, L. R., 1976, “An Extrusion Energy Absorber Suitable for the Protection of Structures during Earthquakes,” Earthquake Engineering and Structural Dynamics, Vol. 4, pp. 251-259

Robinson, W. H., 1982, “Lead-Rubber Hysteretic Bearing Suitable for Protecting Structures during Earthquakes,” Earthquake Engineering and Structural Dynamics, Vol. 10, pp. 593-604.

Shimanoe, S., Hasegawa, K., Kawashima, K. and Shoji, G., 2001, “Dynamic Properties of Rubber-type Shock Absorbers Subjected to Pounding Force,” Proc. Structural and Earthquake Engineering, No. 676/I-55, pp. 219-234, Japan Society of Civil Engineers, Tokyo, Japan (in Japanese).

Skinner, R. V., Robinson, W. H. and McVerry, G. H., 1994, “An Introduction to Seismic Isolation”. John Wiley & Sons, New York, USA

Sugita, H. and Mahin, S., 1994, “Manual for Menshin Design of Highway Bridges: Ministry of Construction, Japan,” Report No. UCB/EERC 94-10, Earthquake Engineering Research Center, University of California, Berkeley, CA, USA.

Technology Research Center for National Land Development, 1989, “Guideline for Seismic Isolation of Highway Bridges,” Tokyo, Japan

Tseng, W.S. and Penzien, J., 1973, “Analytical Investigations of Seismic Response of Long Multi-span Highway Bridges,” Report No. EERC 73-12, Earthquake Engineering Research Center, University of California, Berkeley, CA, USA

Unjoh, S., Kondoh, M. and Okahara, M., 1999, “Development of Displacement Absorption Joint System for Menshin Design,” Proc. International Workshop on Mitigation of Seismic Effects on Transportation Structures, pp. 184-195, Taipei, Taiwan, R.O.C.

Uruta, H., Kawashima, K., Shoji, G. and Sudo, C., 2000, “Evaluation of Stress-Strain Relation for A Rectangular Shock Absorbing Device under An Extreme Compression Stress,” Proc. Structural and Earthquake Engineering, No. 661/I-53, pp. 71-83, Japan Society of Civil Engineers, Tokyo, Japan (in Japanese).